SAND2014-1478P

Exceptional service in the national interest

Sandia National Laboratories

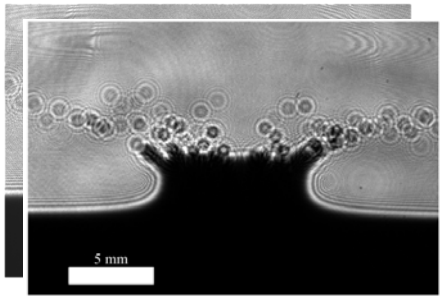

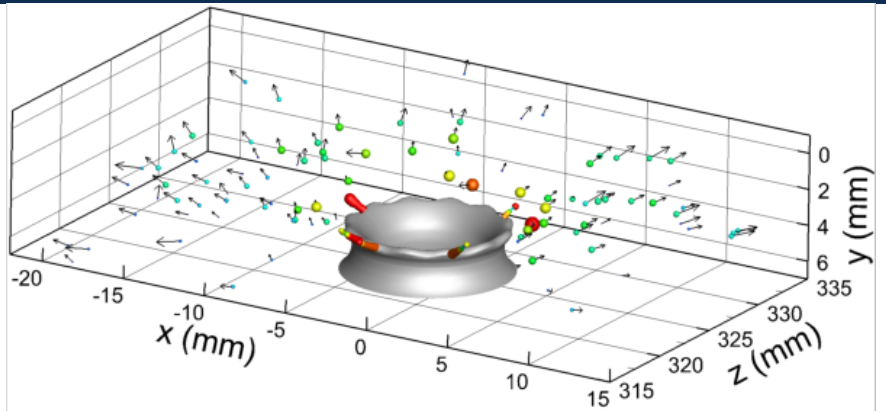

Digital in-line holography for 3D quantification of complex multiphase flows

Daniel R. Guildenbecher

March 3, 2014

U.S. DEPARTMENT OF ENERGY
NNSA National Nuclear Security Administration

Sandia National Laboratories is a multi-program laboratory managed and operated by Sandia Corporation, a wholly owned subsidiary of Lockheed Martin Corporation, for the U.S. Department of Energy's National Nuclear Security Administration under contract DE-AC04-94AL85000.

Motivation: Multiphase fragmentation

Sandia National Laboratories

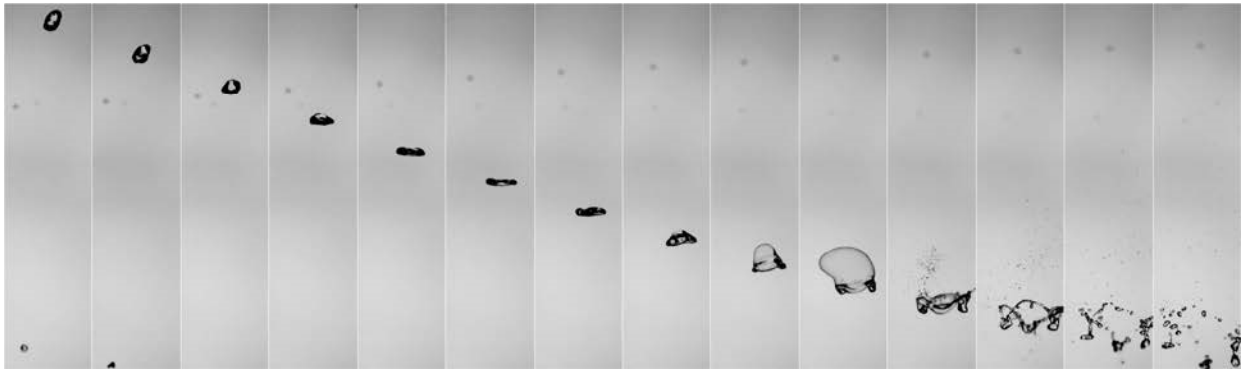

Villermaux and Bossa, 2009, *Nature Physics*

http://www.michiganfiresprinkler.com/images/sprinklerheadgoingoff_0sh6_g76y_8uzb.bmp

http://z.about.com/d/autorepair/1/0/O/3/-/-/diesel-cutaway-bosch.jpg

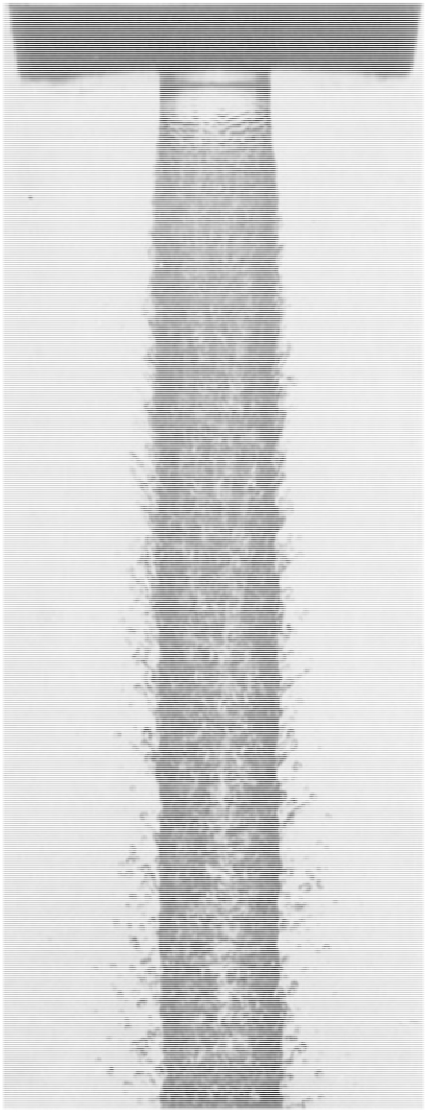

Hoyt and Taylor, 1977,
J. Fluid Mech.

Motivation: Trend toward 3D prediction

Sandia National Laboratories

1878

Lord Rayleigh, *Proc. Lond. Math. Soc.*

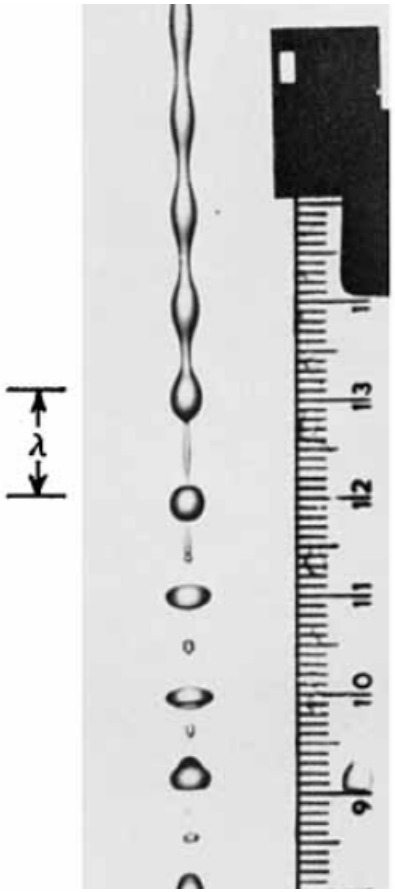

Rutland and Jameson 1971, *J.Fluid Mech.*

1987

O'Rourke, and Amsden, *Proc. SAE*

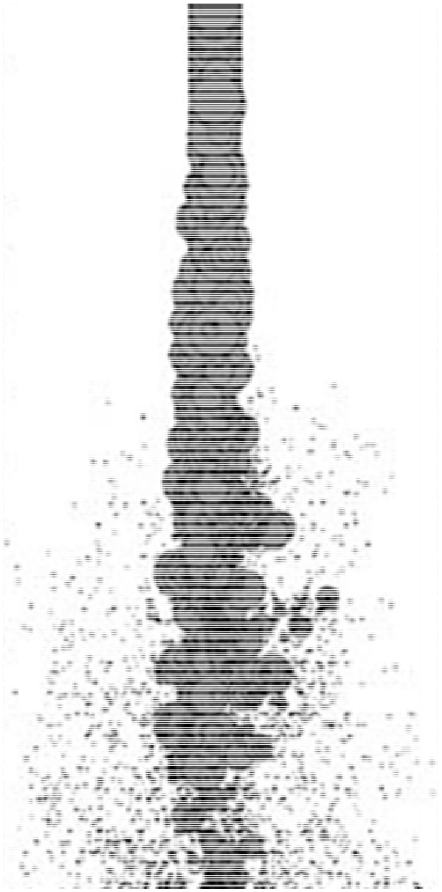

Apte et al, 2009, *Proc. Combustion Institute*

2004

Yoon and Heister, *Phys. Fluids*

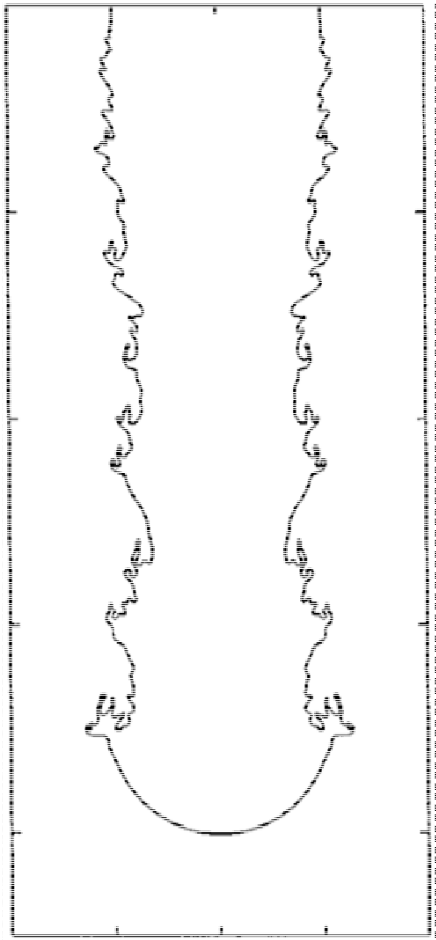

2007

Ménard et al., *Int. J. Multiphase Flow*

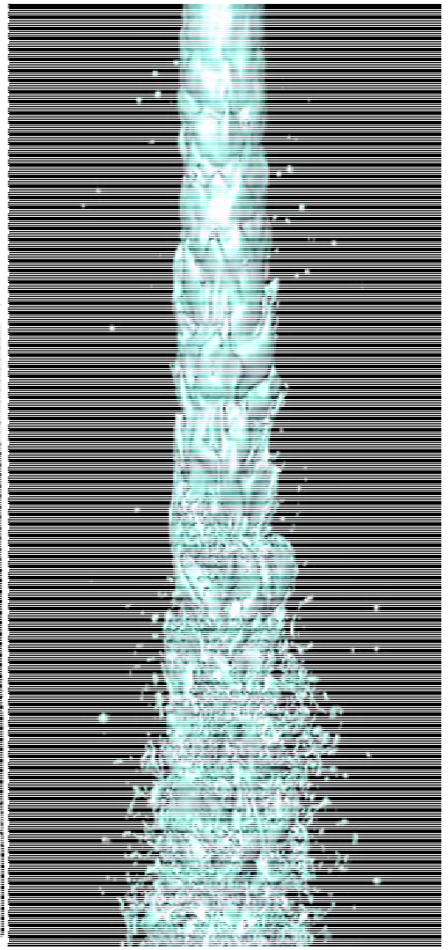

Motivation: 3D imaging for a 3D world

Challenge: 2D imaging or point-wise measurements cannot resolve 3D flow phenomena

- Repetition needed to capture spatial statistics

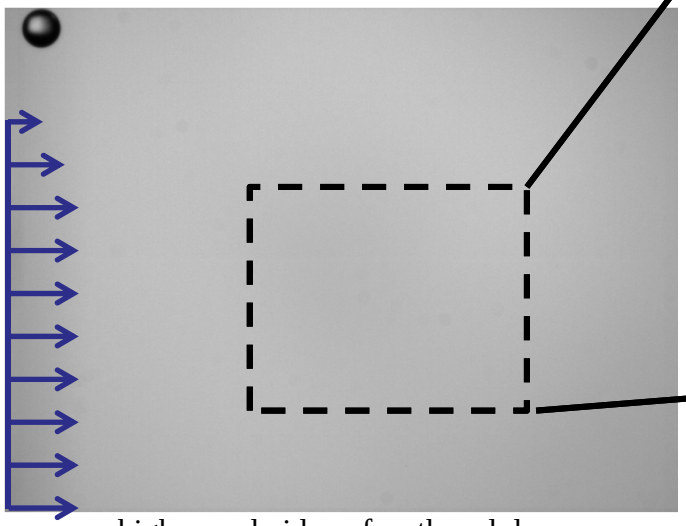

high-speed video of a ethanol drop in an air-stream

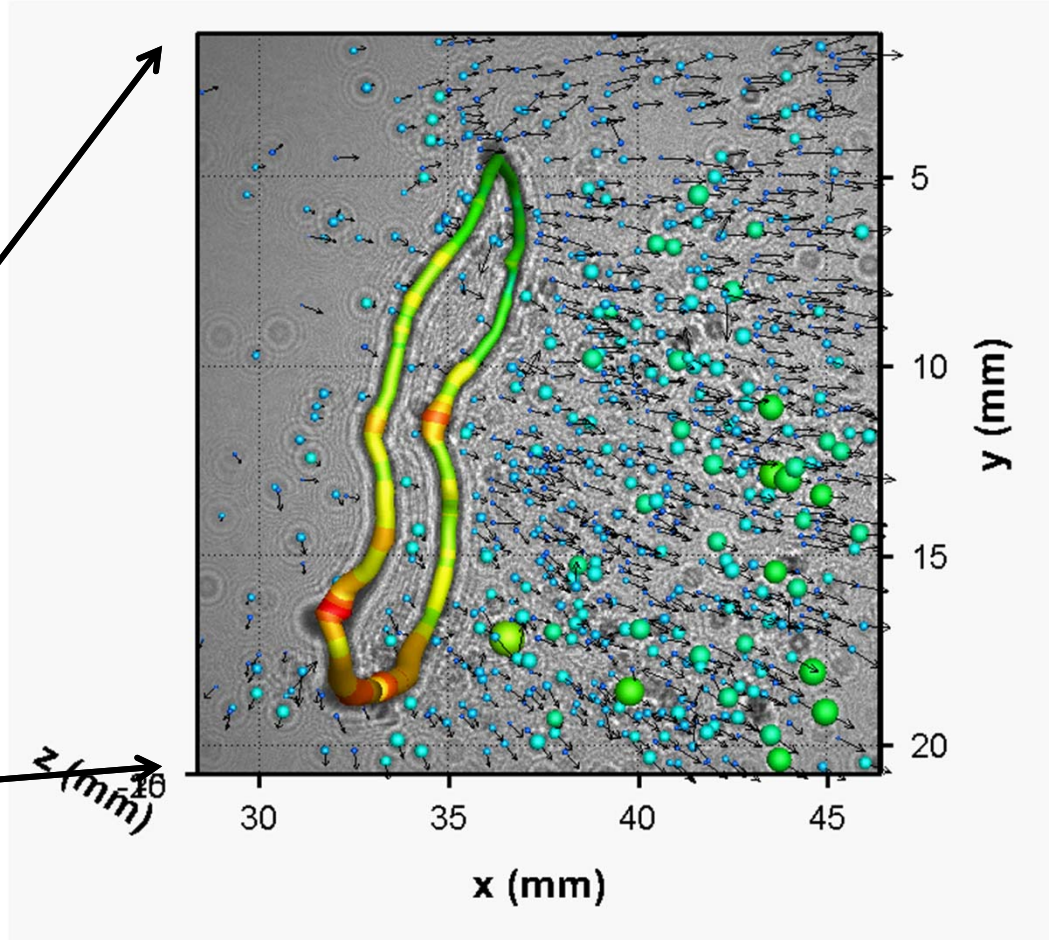

digital holographic measurement
(Gao, Guildenbecher et al, 2013, *Opt. Lett.*)

Holography is an optical technique to record and reconstruct a 3D light field

- Applications include sprays, high-speed particle fields, fluid-flow measurements, droplet combustion, etc…

What is holography?

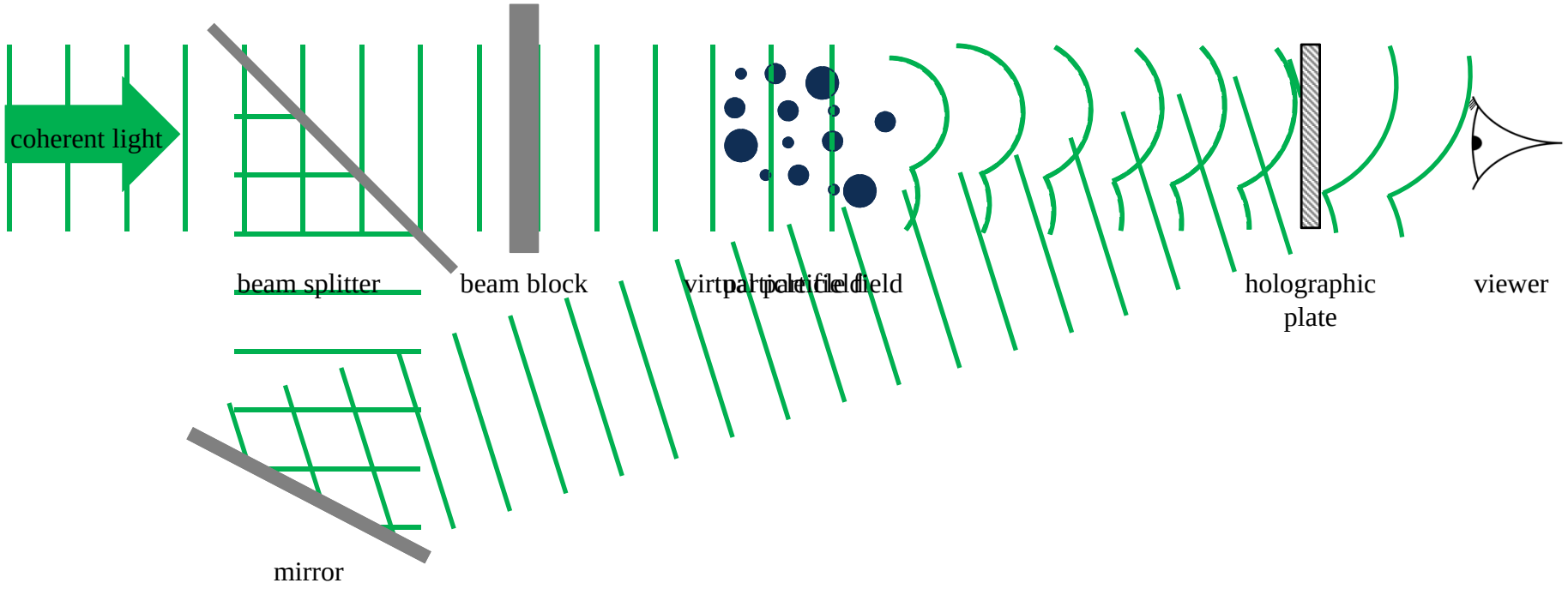

Optical method first proposed by Gabor in 1948

1. Coherent light scattered by particle field forms the object wave, E_o
2. Interference with a reference wave, E_r, forms the hologram: $h = |E_o+E_r|^2$
3. Reconstruction with E_r forms virtual images at original particle locations

$$h \cdot E_r = \underbrace{(|E_o|^2 + |E_r|^2)E_r}_{\text{DC term}} + \underbrace{|E_r|^2 E_o}_{\text{virtual image}} + \underbrace{E_r^2 E_o^*}_{\text{real image}}$$

Digital in-line holography (DIH)

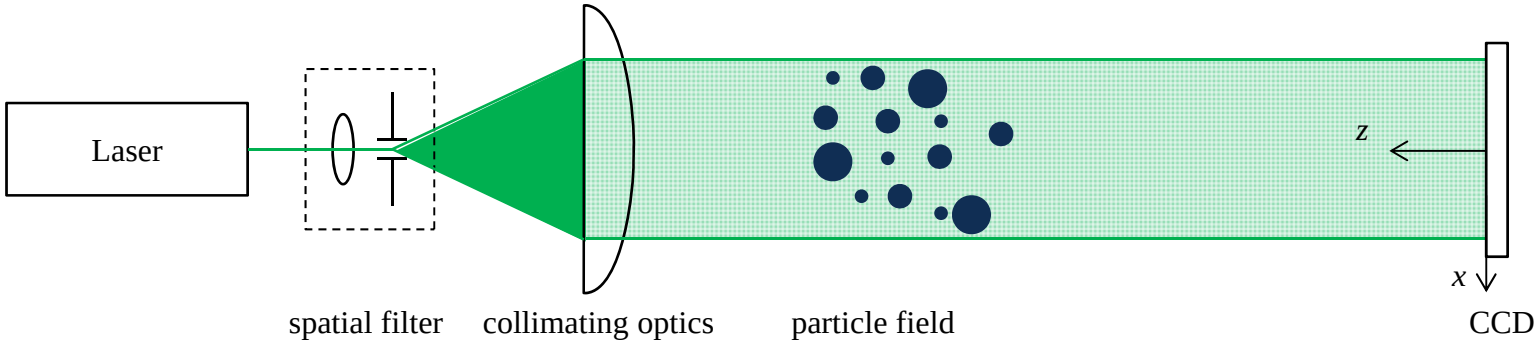

Holographic plate and cumbersome wet-chemical processing replaced with digital sensor (CCD or CMOS)

- Resolution of digital sensors (order 100 line pairs/mm) is much less than resolution of photographic emulsions (order 5,000 line pairs/mm)
  - For suitable off axis angles, θ, the fringe frequency, f, is typically too large to resolve with digital sensors ($f = 2\sin(\theta/2)/\lambda$)
- Rather, the in-line configuration ($\theta = 0$) is typically utilized
  - Reference wave is that portion of the beam which passes through the particle field undisturbed
  - **Consequently, the real image overlaps with an out-of-focus virtual image**

Digital in-line holography (DIH)

- In the computer, we multiply the digitally recorded hologram *h* by an estimate of the complex conjugate of the reference wave E_r^*

$$h \cdot E_r^* = \underbrace{(|E_o|^2 + |E_r|^2)E_r^*}_{\text{DC term}} + \underbrace{E_r^{*2}E_o}_{\text{virtual image}} + \underbrace{|E_r|^2 E_o^*}_{\text{real image}}$$

- This complex amplitude can be numerically propagated to any distance along the optical axis, z, using the diffraction equations

$$E(x,y,z) = h(x,y) \cdot E_r^*(x,y) \otimes g(x,y,z)$$

  - Rayleigh-Sommerfeld: $g(x,y,z) = e^{jk\sqrt{x^2+y^2+z^2}} \Big/ j\lambda\sqrt{x^2+y^2+z^2}$
  - Fresnel-Kirchhoff: $g(x,y,z) = \frac{e^{jkz}}{j\lambda z} e^{jk\left(x^2+y^2\right)/2z}$

- Numerically, the convolution is computed using the fast Fourier transform (FFT)

$$E(x,y,z) = FFT^{-1}\left\{FFT\left\{I_0(x,y)E_r^*(x,y)\right\}FFT\left\{g(x,y,z)\right\}\right\}$$

- Visualized via the reconstructed amplitude, $A = |E|$, or intensity, $I = |E|^2$

Digital in-line holography (DIH)

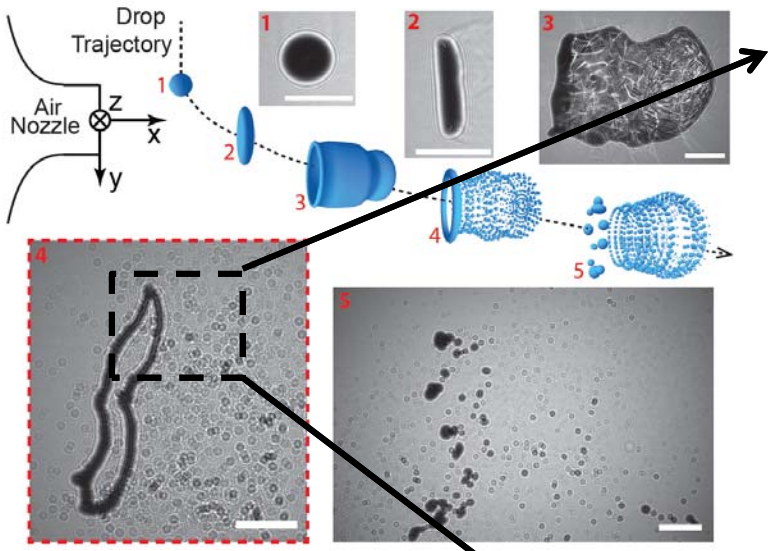

digital holograms of the breakup of an ethanol drop in an air-stream (Gao, Guildenbecher et al 2013, *Opt. Lett.*)

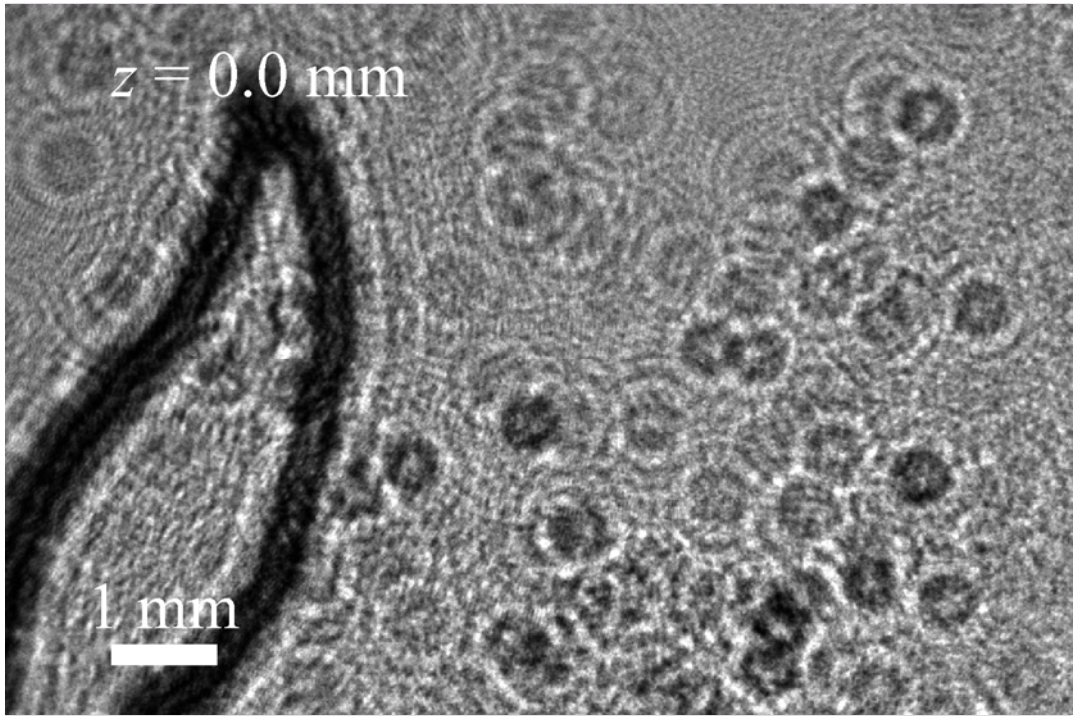

Reconstructed amplitude throughout depth, *z*

- In-focus structures are clearly observed at different depths, *z*
- "Rings" around the in-focus structures are the out-of-focus virtual images

Challenge: How can we automatically extract in-focus objects?

The depth-of-focus problem

The spatial extent of the diffraction pattern limits the angular aperture, Ω, from which a particle is effectively reconstructed (Meng et al, 2004, *Meas. Sci. Technol.*):

- From the central diffraction lobe → $\Omega \approx 2\lambda/d$
- Using the traditional definition of depth-of-focus, δ, based on change of intensity within the particle center → $\delta \approx 4\lambda/\Omega^2$
- Therefore: for in-line holography, $\delta \approx d^2/\lambda$
  - Example: d = 465 μm, λ = 532 nm → $\delta \approx$ 400 mm!

Literature contains two basic methods to find the focal plane with improved accuracy:

1. Fit a model to the observed diffraction patterns (inverse method)
   - Generally accurate with small depth uncertainty
   - Limited to objects with known diffraction patterns (spheres)
2. Reconstruct the amplitude (or intensity) throughout depth and apply a focus metric to find "in-focus" objects
   - No *a-priori* knowledge of particle shape required
   - Accuracy is a strong function of the chosen focus metric

Example: Tian et al (2010)

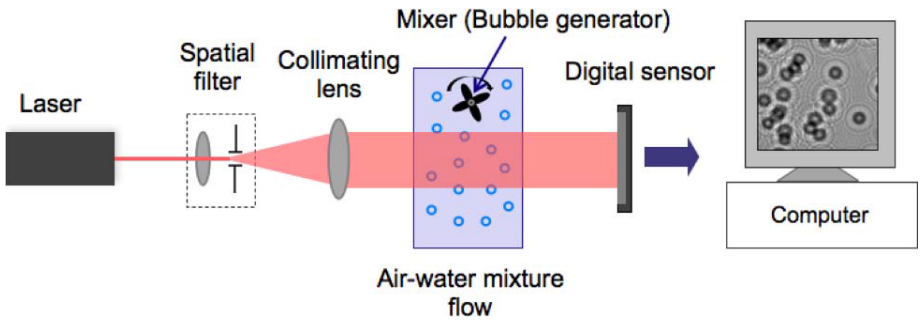

Experimental configuration

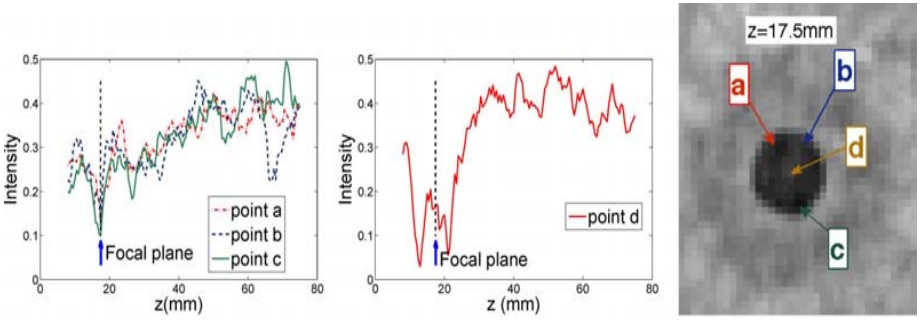

Focus criteria

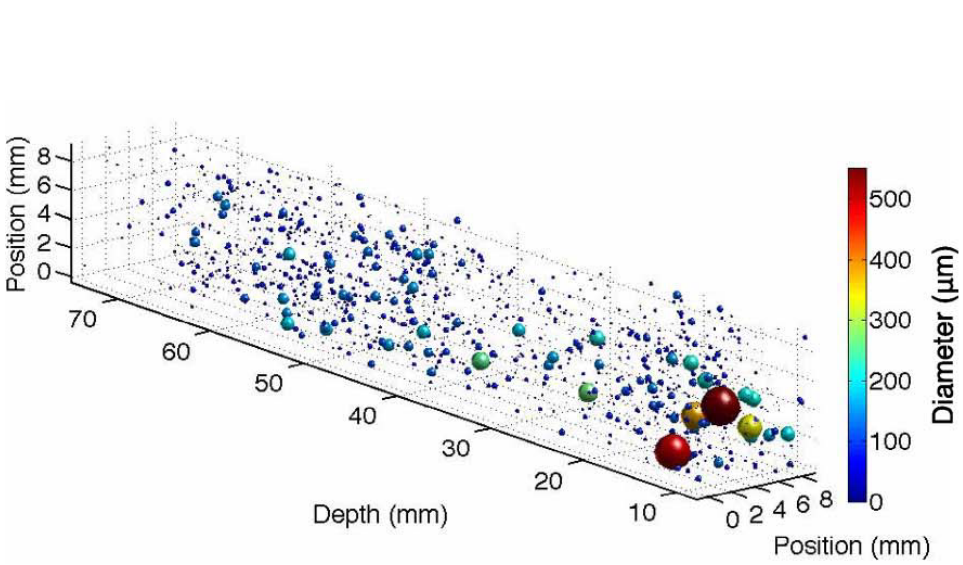

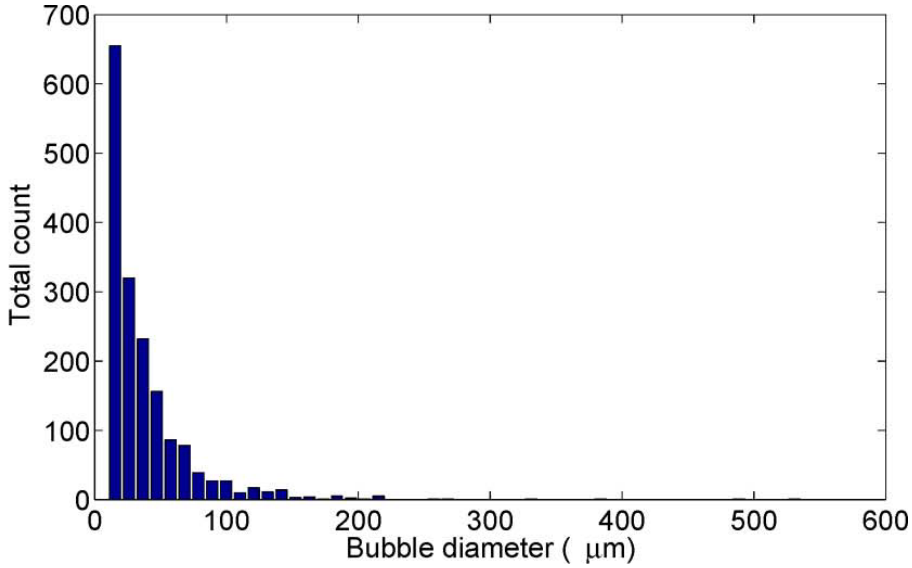

Experimental results

Issue: Validated accuracy is needed for quantitative diagnostics

Single particle simulations

Simulations produce holograms with known properties

- Non-spherical shapes can be considered
- Details in Guildenbecher et al, 2013, *Appl. Opt.*

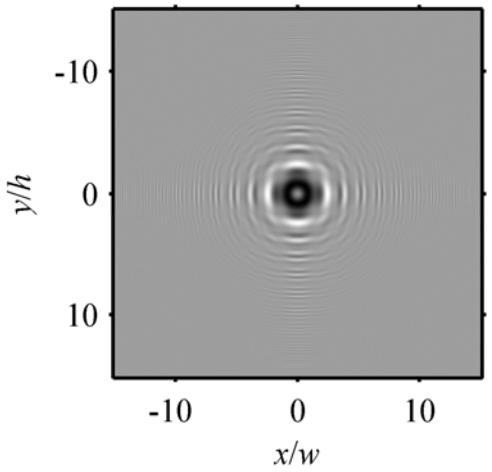

Simulated hologram of a square

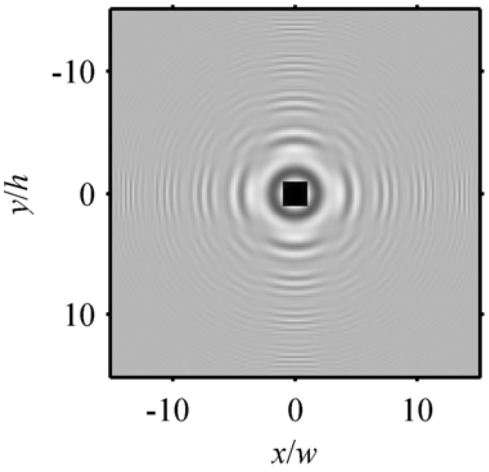

Reconstruction at $Z = Z_o$

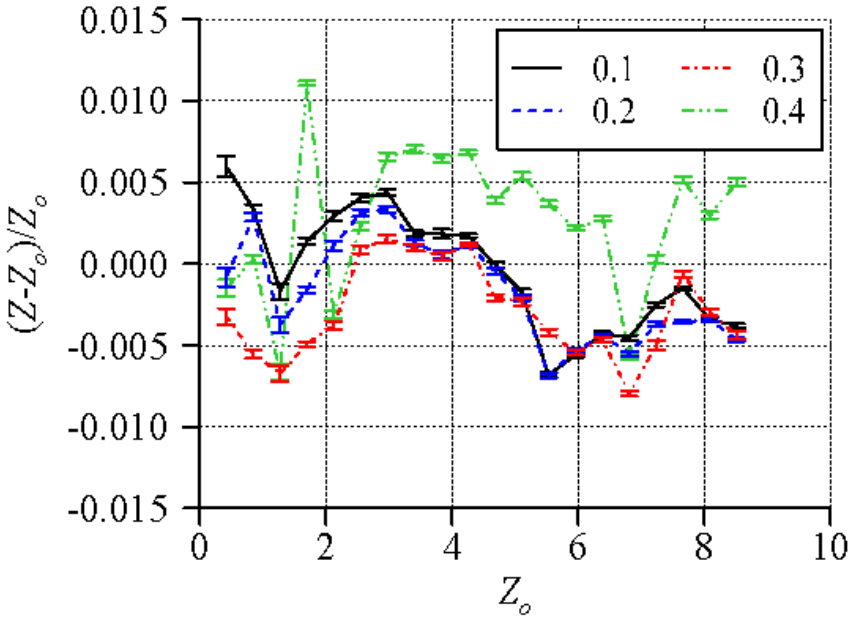

Depth uncertainty as a function of non-dimensional particle distance, Z_o, and segmentation threshold

Challenges in existing particle extraction methods:

- Optimum segmentation threshold is not known *a-priori*
- Results are unstable with respect to particle position, Z_o

Hybrid particle extraction method

Sandia National Laboratories

Basic idea: In-focus regions display a minimum amplitude within the particle interior and a maximum sharpness at the particle edges

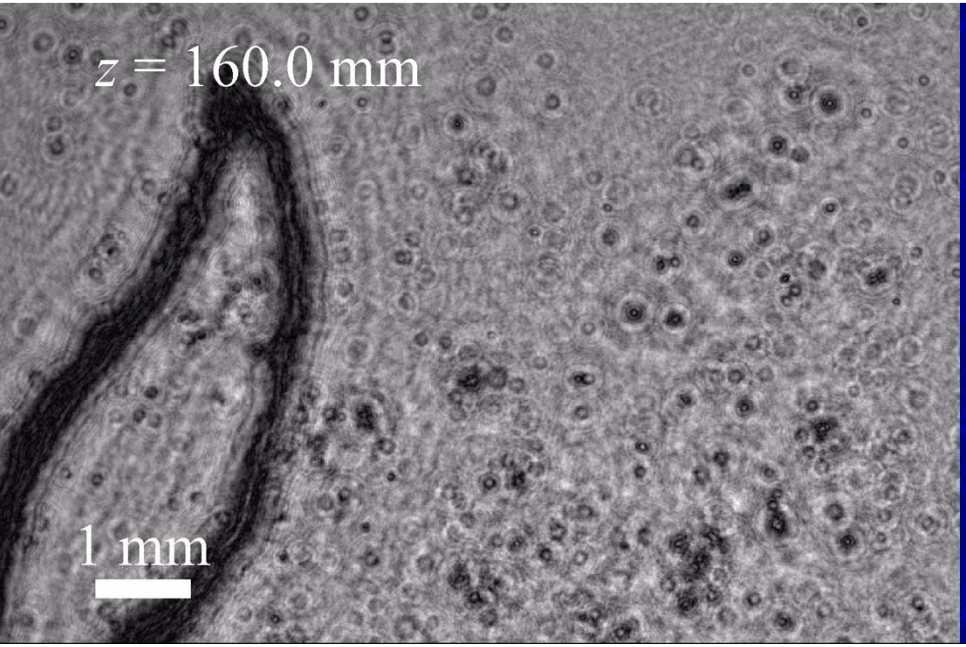

Reconstructed amplitude throughout depth, *z*

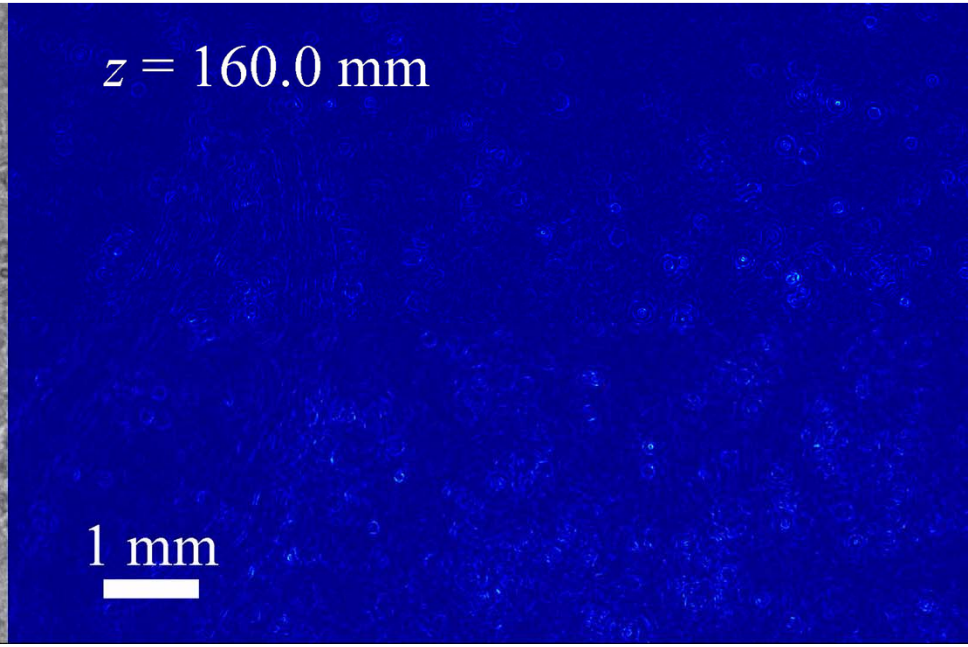

Reconstructed edge sharpness throughout depth, *z*

- Optimum segmentation threshold is automatically extracted from the threshold of the amplitude which displays maximum edge sharpness
  - Further details in Guildenbecher et al, 2013, *Appl. Opt.* and Gao, Guildenbecher, et al, 2013, *Opt. Express.*

Hybrid particle extraction method

Simulations indicate improved accuracy

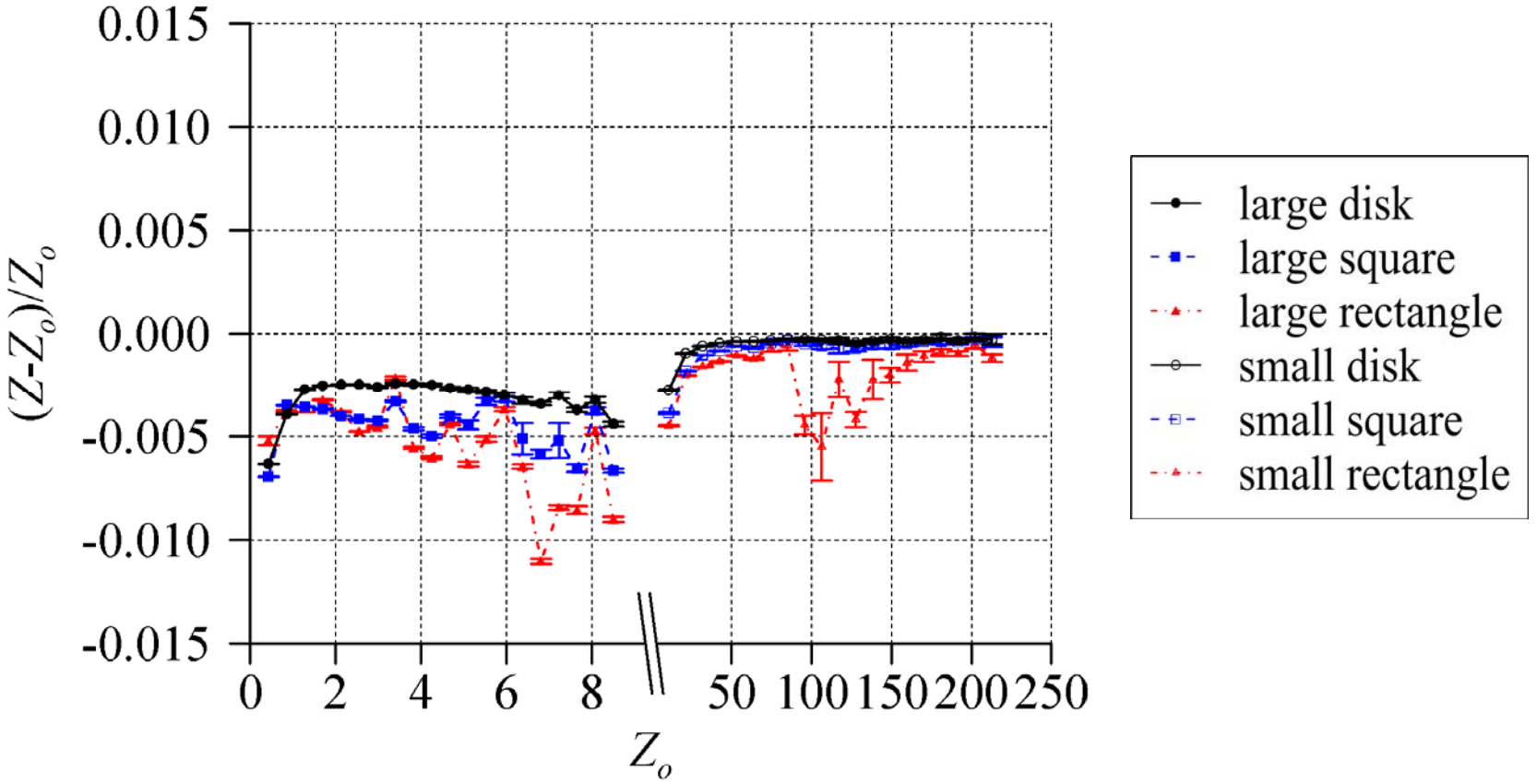

Depth uncertainty for hybrid method

Simulations provide a theoretical best case scenario. Experiments are needed to quantify real world challenges

Experimental validation

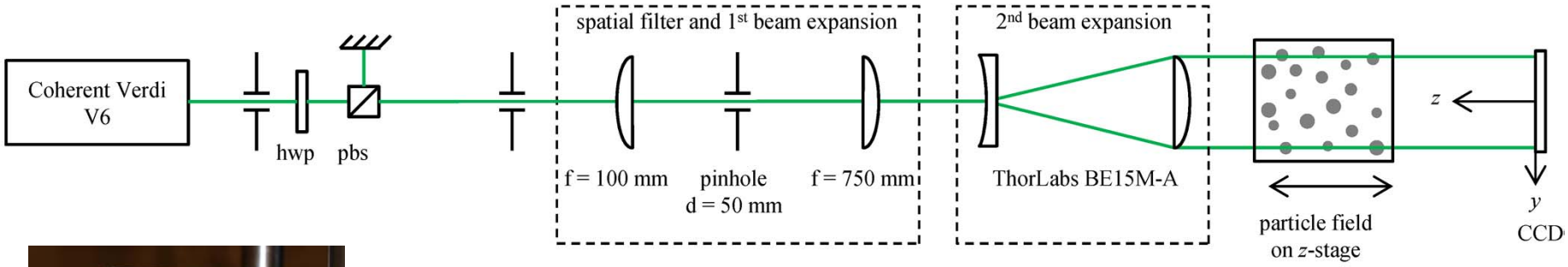

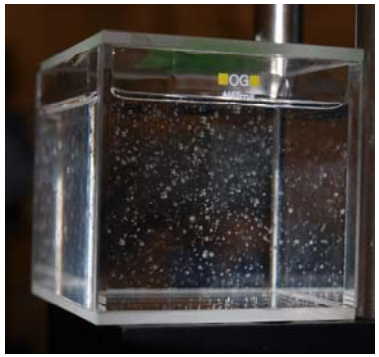

particle field

- Quasi-stationary particle field
  - Polystyrene beads ($\bar{d} \approx 465\,\mu m$) in 10,000 cSt silicone oil
  - Settling velocity ≈ 0.8 mm/s
- Multiple holograms recorded, displacing the particle field 2 mm in the *z*-direction between each acquisition

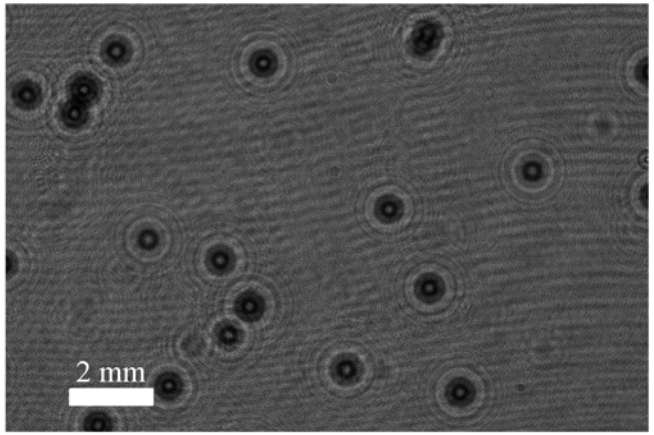

hologram

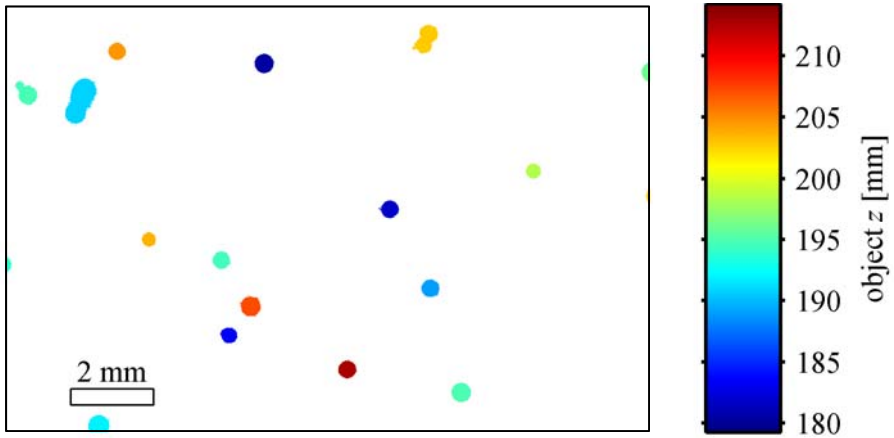

Detected objects colored by *z*-position

Experimental validation

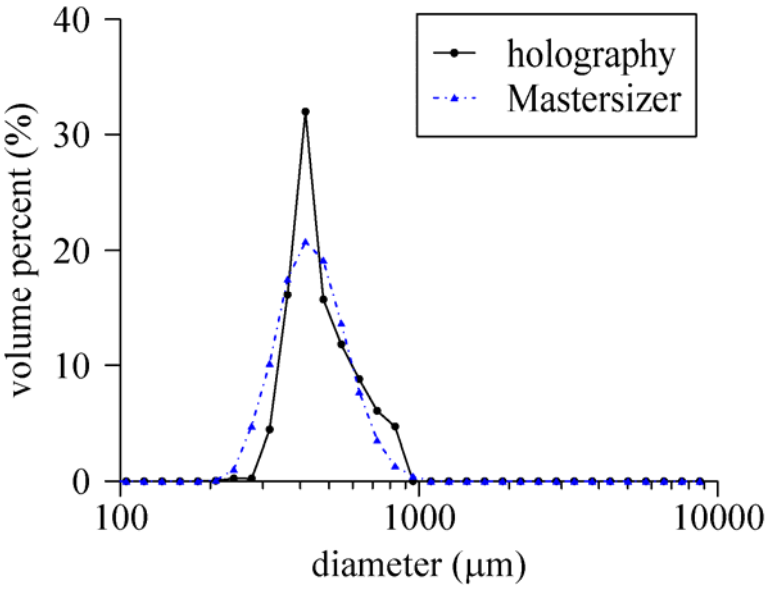

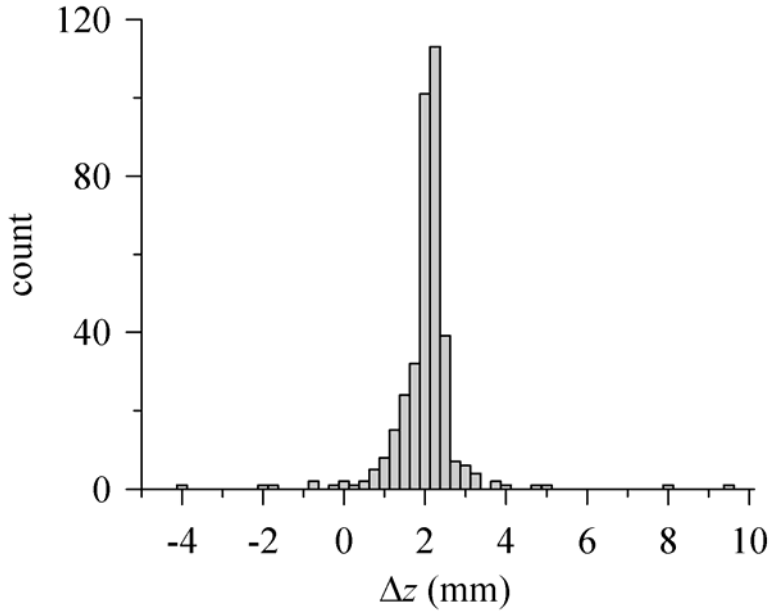

Diameter measured from area of the detected 2D morphology

- Actual mass median diameter = 465 μm
- Measured mass median diameter = 474 μm
  - Error of 2.0% with respect to actual value

Displacement found by particle matching between successive holograms

- Actual displacement = 2.0 mm
- Mean detected displacement = 1.91 mm +/- 0.81 mm
  - Standard deviation of 1.74 times mean diameter

Aerodynamic drop fragmentation

Sandia National Laboratories

Motivation: fundamental spray process and an important canonical problem for multiphase simulations

- No viable methods to measure secondary drop size/velocity statistics or the 3D morphology of the ring shaped ligament

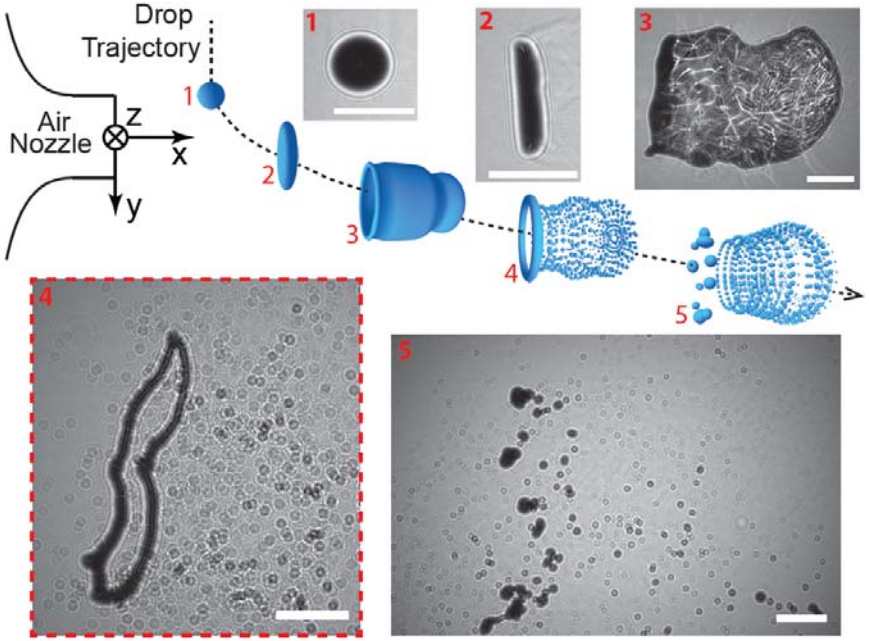

digital holograms of the breakup of an ethanol drop in an air-stream (Gao, Guildenbecher et al 2013, *Opt. Lett.*)

Experimental configuration: Double-pulsed laser and imaging hardware as typically used in PIV

- λ = 532 nm, 5 ns pulsewidth
- Interline transfer CCD (4008 × 2672, 9 μm pixel pitch)
- Temporal separation, Δt = 62 μs, determined by laser timing
  - Note: experiments in Guildenbecher et al, 2013, *Proceedings of Digital Holography and 3-D Imaging* confirm no loss of accuracy due to the reduced coherence length of these lasers

Aerodynamic drop fragmentation

- Secondary drop sizes/positions extracted by the hybrid method
  - Comparison with phase Doppler anemometer (PDA) data confirms accuracy of measured sizes

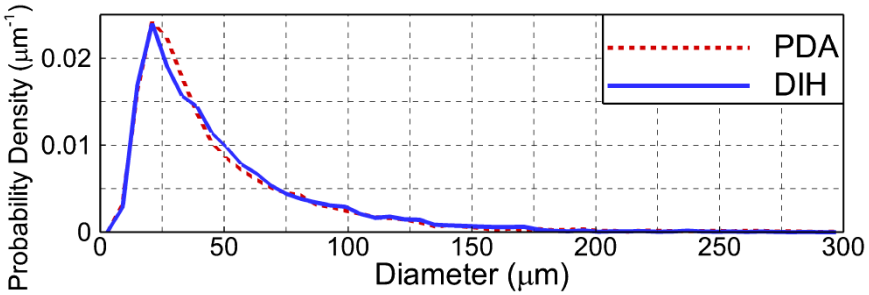

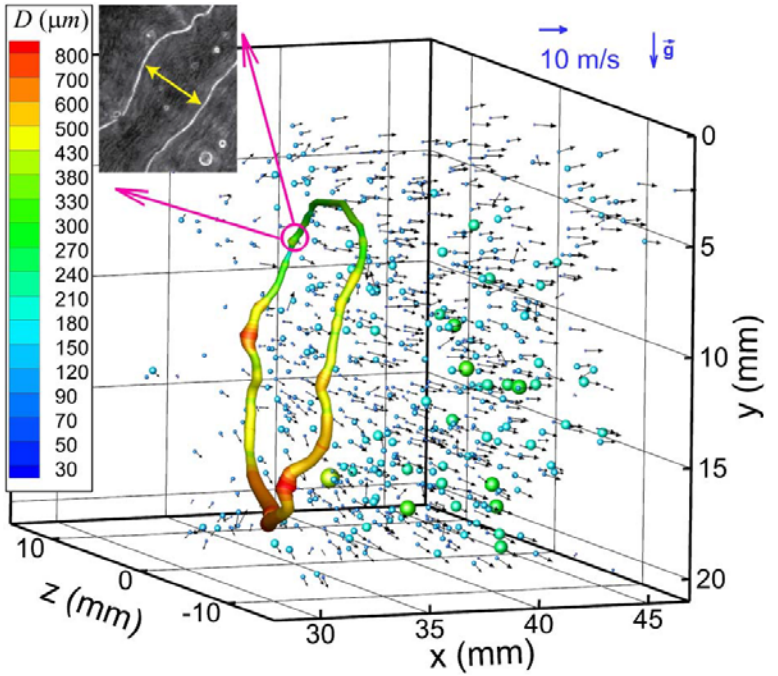

- Ring measured from *z*-location of maximum edge sharpness
  - Total volume of ring + secondary drops is within 2.2% of the initial volume
- 3C velocity measured by particle matching between successive frames
  - Expected symmetry observed with higher uncertainty in *z*-direction

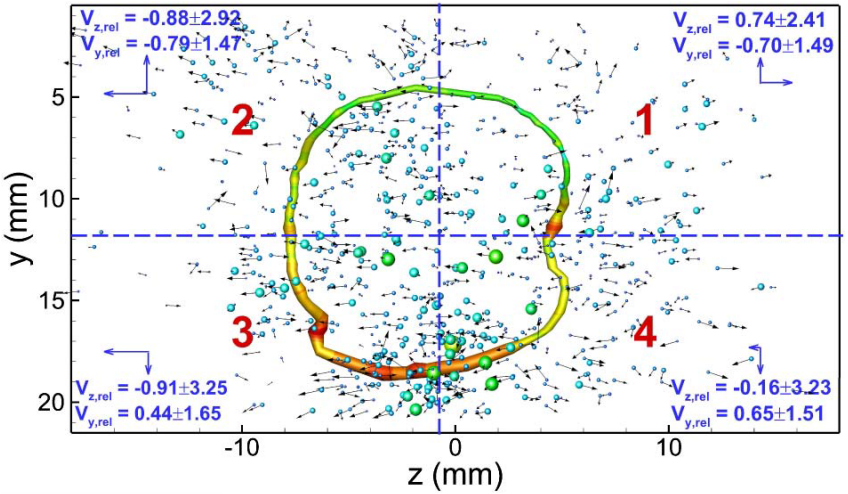

Drop impact on a thin film

Sandia National Laboratories

Motivation: measurement of secondary droplet by other methods requires significant experimental repetition

- Process symmetry provides opportunities to validate accuracy

Experimental configuration:

- Double pulsed laser (λ = 532 nm, 5 ns pulsewidth)
- Interline transfer CCD (4872 × 3248, 7.4 μm pixel pitch)
- Temporal separation, Δt = 33 μs, determined by laser timing

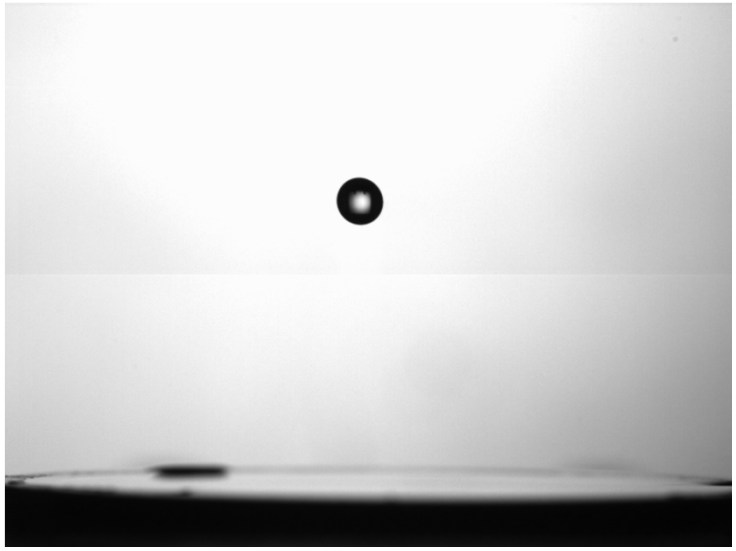

impact of a 3 mm water drop on a 2 mm water film (Guildenbecher et al, 2013, *Exp. Fluids*.)

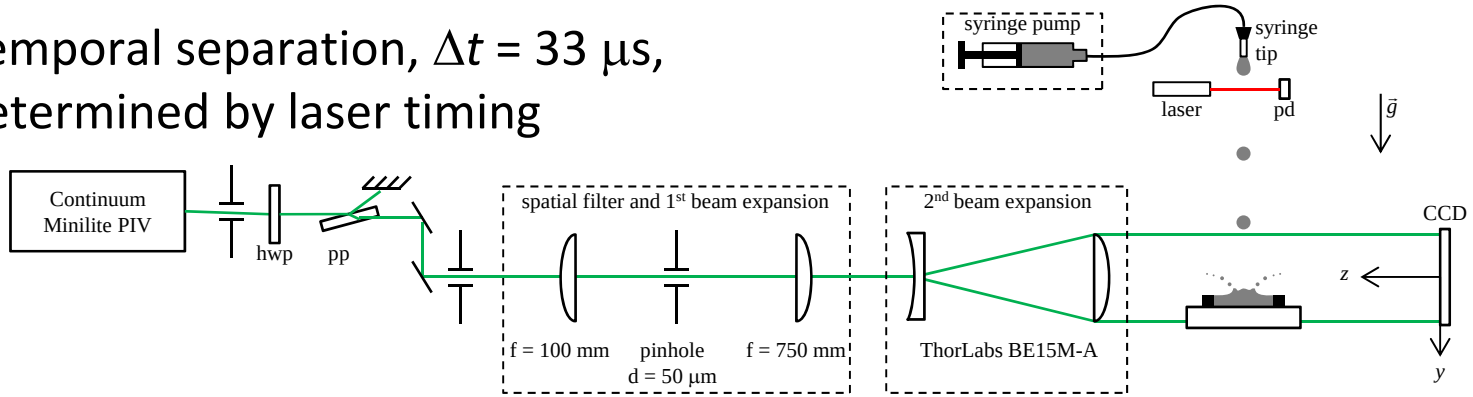

experimental configuration of holographic recording of drop impact on a thin film (Guildenbecher et al, 2014, *Exp. Fluids*.)

Drop impact on a thin film

Sandia National Laboratories

Again processed with the hybrid method

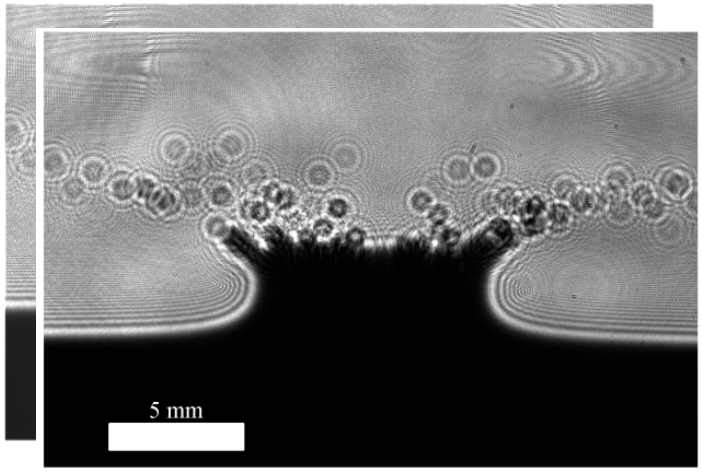

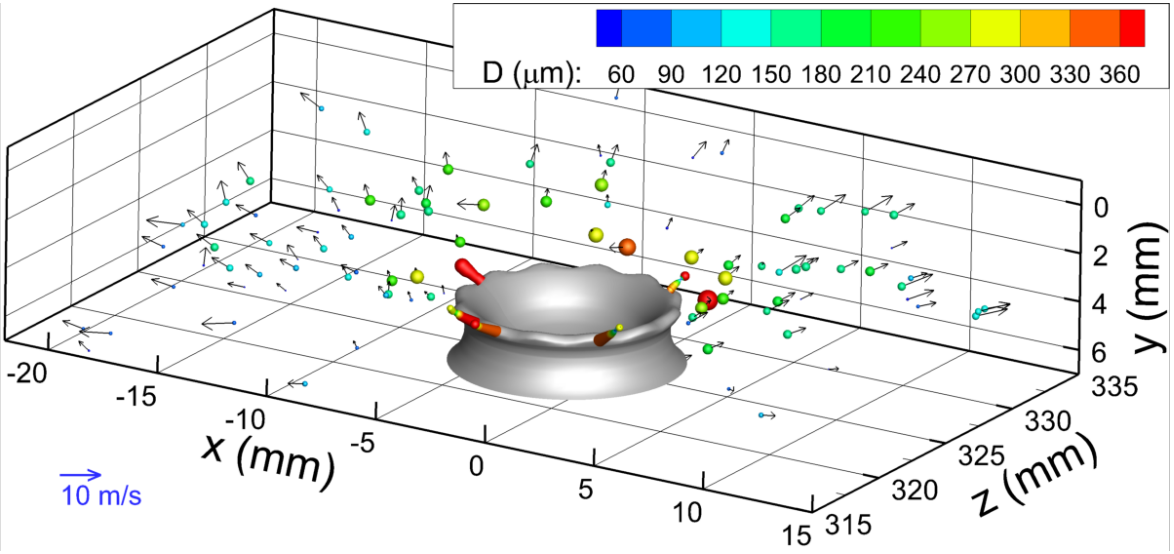

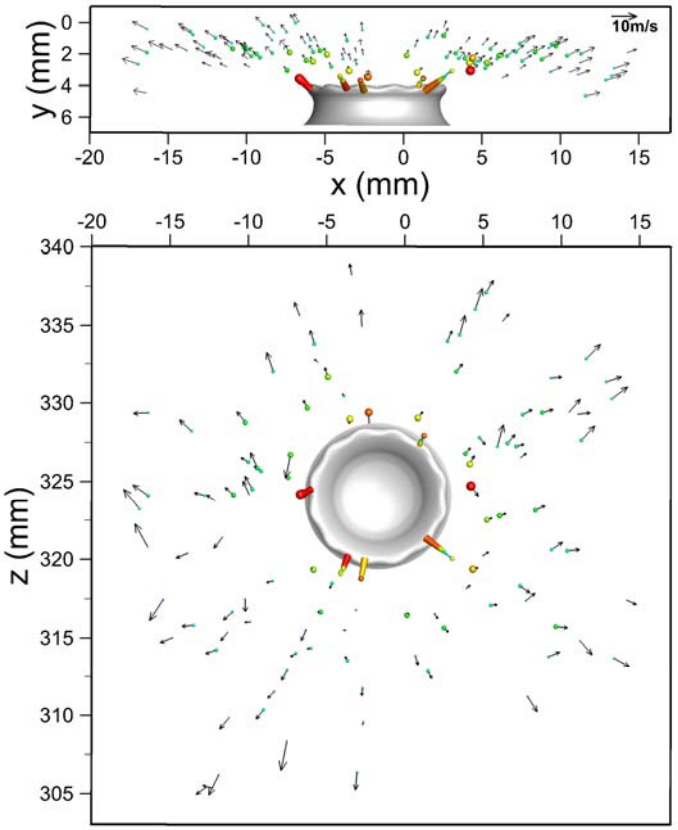

holographic reconstruction of
drop impact on a thin film
(Guildenbecher et al, 2014, *Exp. Fluids*.)

Drop impact on a thin film

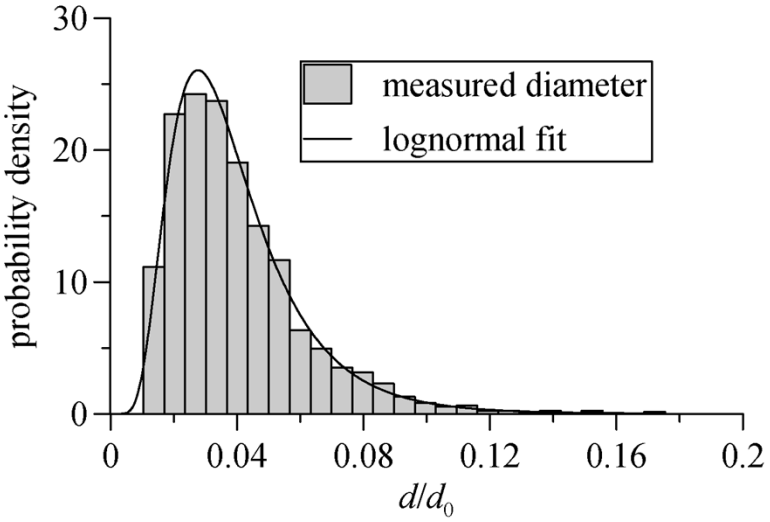

Drop size distribution shows the expected lognormal behavior

- Probability goes to zero at large and small diameters

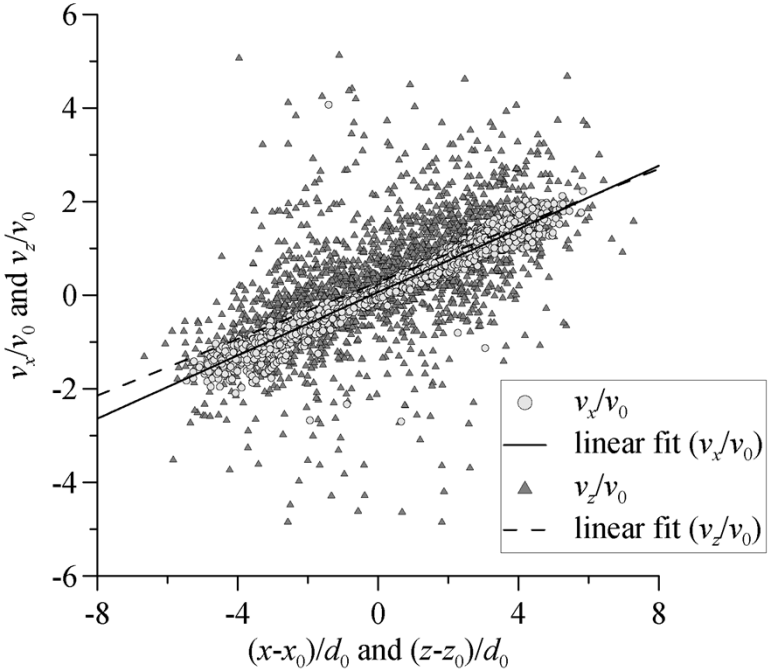

Symmetry in the in-plane (v_x) and out-of-plane (v_z) velocities confirms accuracy in measured v_z

- Difference in scatter gives estimated z-uncertainty of $0.72 \cdot \overline{d}$

Sonic pellets from a shotgun

Sandia National Laboratories

Motivation: a shotgun simulates blast environments

Challenge: Shock-waves introduce noise

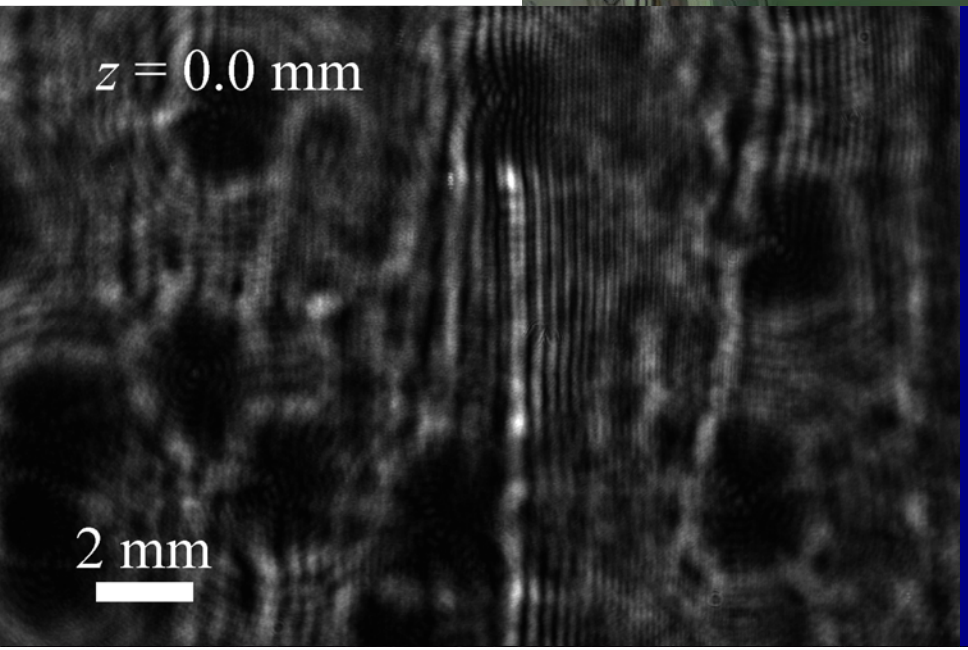

Reconstructed amplitude throughout depth, z

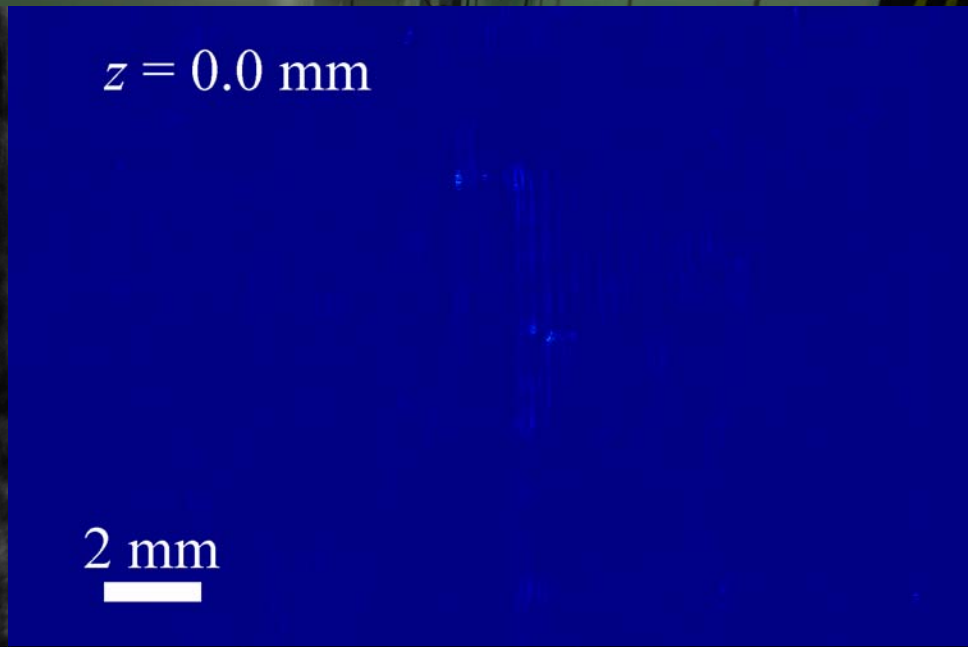

Reconstructed edge sharpness throughout depth, z

Holography configuration for shotgun investigations

Cross-correlation method

Sandia National Laboratories

Theory: in-focus particle images from two sequential holograms contain correlated information

- The maximum cross-correlation, c, gives the displacement (Δx, Δy)

$$c = \max_{\Delta x, \Delta y}\left[\sum_m \sum_n \mathrm{Img}_1(m,n)\,\mathrm{Img}_2^*(m,n)(m-\Delta x, n-\Delta y)\right]$$

- Img_1 and Img_2 chosen as the edge sharpness images from the two frames
- z positions in each frame (z_1 and z_2) are found from the maximum value of c over all possible combinations of z_1 and z_2

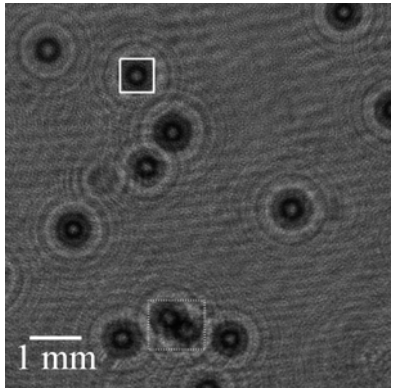

hologram (Guildenbecher et al, 2013, *Opt. Lett.*)

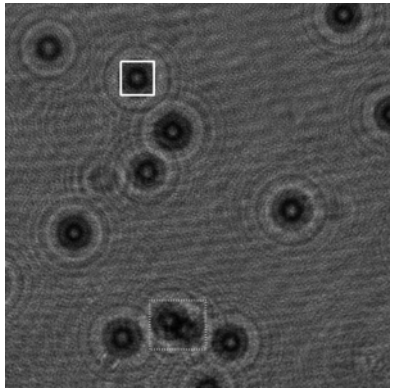

hologram after displacing the particle field by 2 mm (Guildenbecher et al, 2013, *Opt. Lett.*)

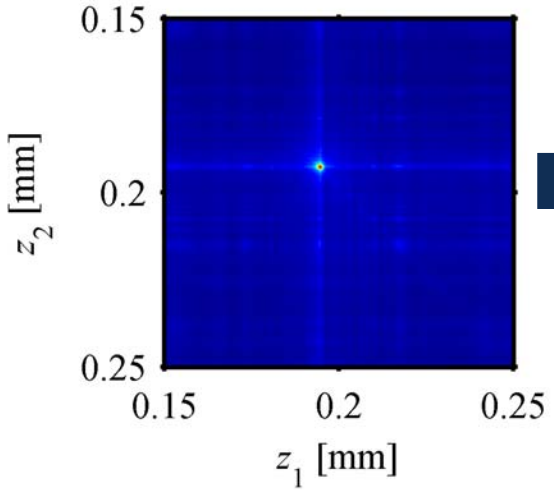

maximum value of c for the particle in the white boxes (Guildenbecher et al, 2013, *Opt. Lett.*)

z_1 = 194.72 mm,
z_2 = 192.72 mm,
Δz = 2.00 mm

Cross-correlation method

Sandia National Laboratories

Again, experimentally validated with quasi-stationary particles in silicone oil

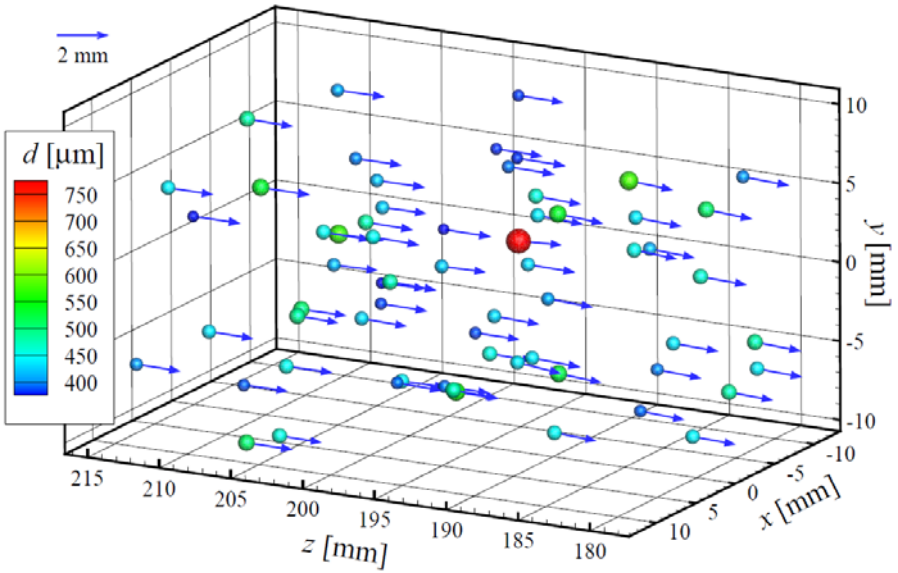

measured displacement field from one realization
(Guildenbecher et al, 2013, *Opt. Lett.*)

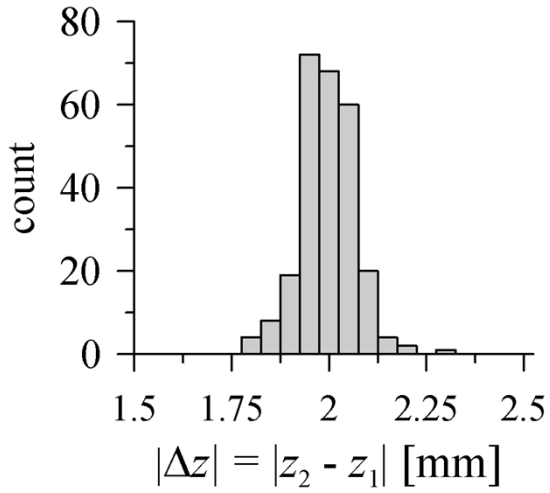

measured *z*-displacements from all realizations
(Guildenbecher et al, 2013, *Opt. Lett.*)

- Actual displacement = 2.0 mm
- Mean detected displacement = 1.996 mm +/- 0.072 mm
  - Standard deviation of 0.15 times mean diameter
  - Order of magnitude improvement compared to uncertainties in the literature

Sonic pellets from a shotgun

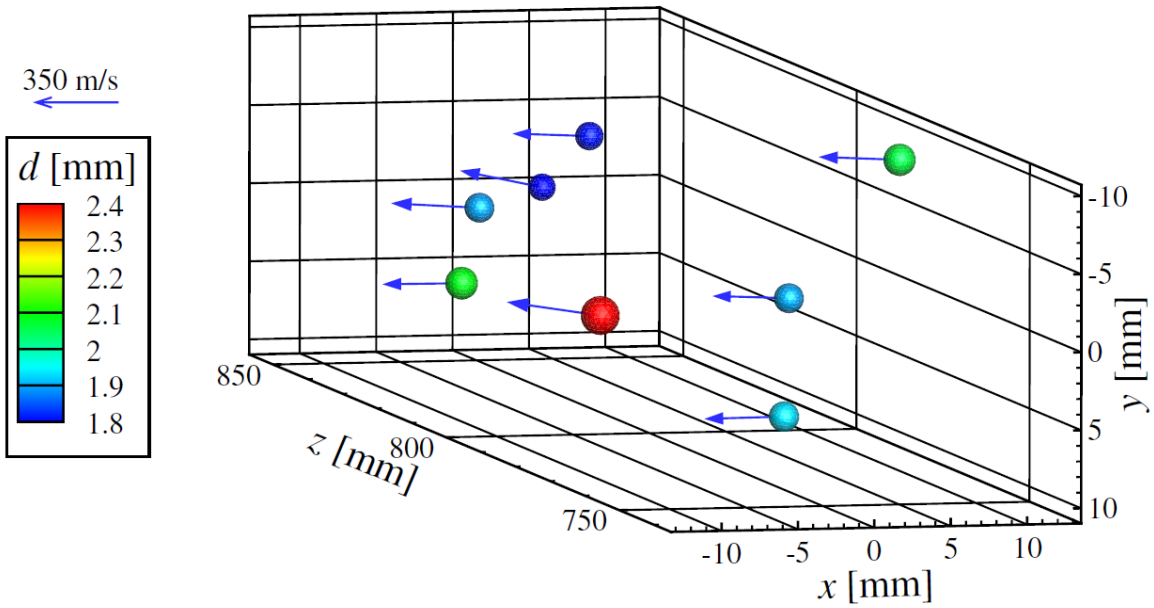

particle field from the shotgun measured with the cross-correlation method
(Guildenbecher et al, 2013, *Opt. Lett.*)

Results closely match the expected mean velocity (350 m/s) and diameter (2.0 mm)

- Uncertainty in Δz is on the order of 0.2 particle diameters

Aluminum drop combustion in propellants

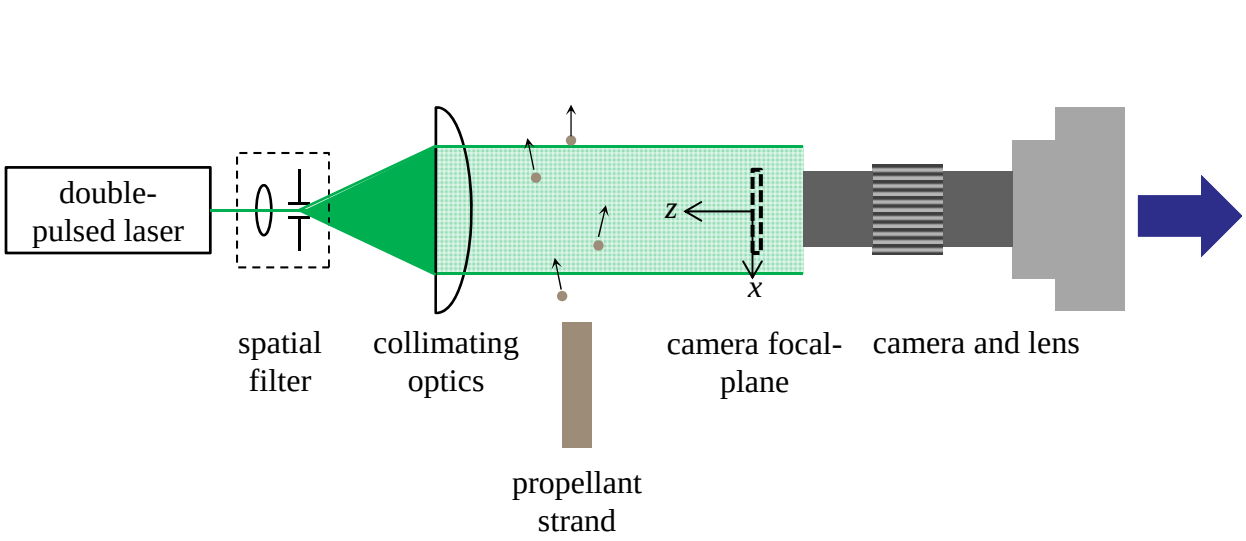

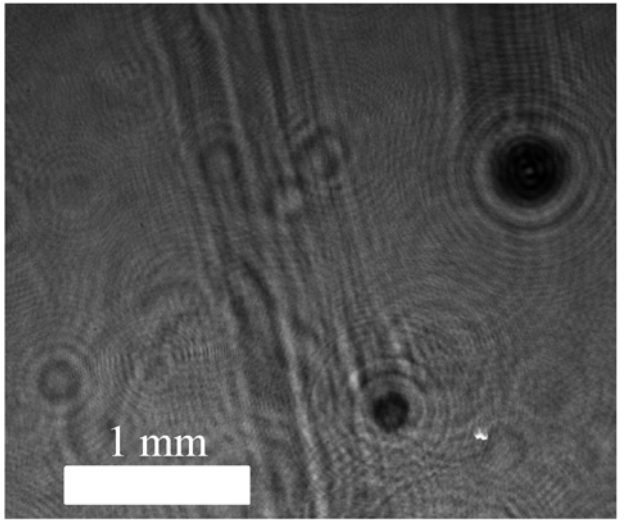

recorded hologram

Propellant: solid-rocket propellant pressed into a strand roughly 5 mm in diameter and initially 10 cm long

- Combusts from the top surface down, ejecting molten aluminum particles traveling on the order of 10 m/s

Laser: Continuum Minilite Nd:YAG, 532 nm wavelength, 5 ns pulse duration

Camera: sCMOS from LaVision at 15Hz

Lens: Infinity K2 long distance microscope with CF-4 objective

- ~ 6X magnification

Aluminum drop combustion in propellants

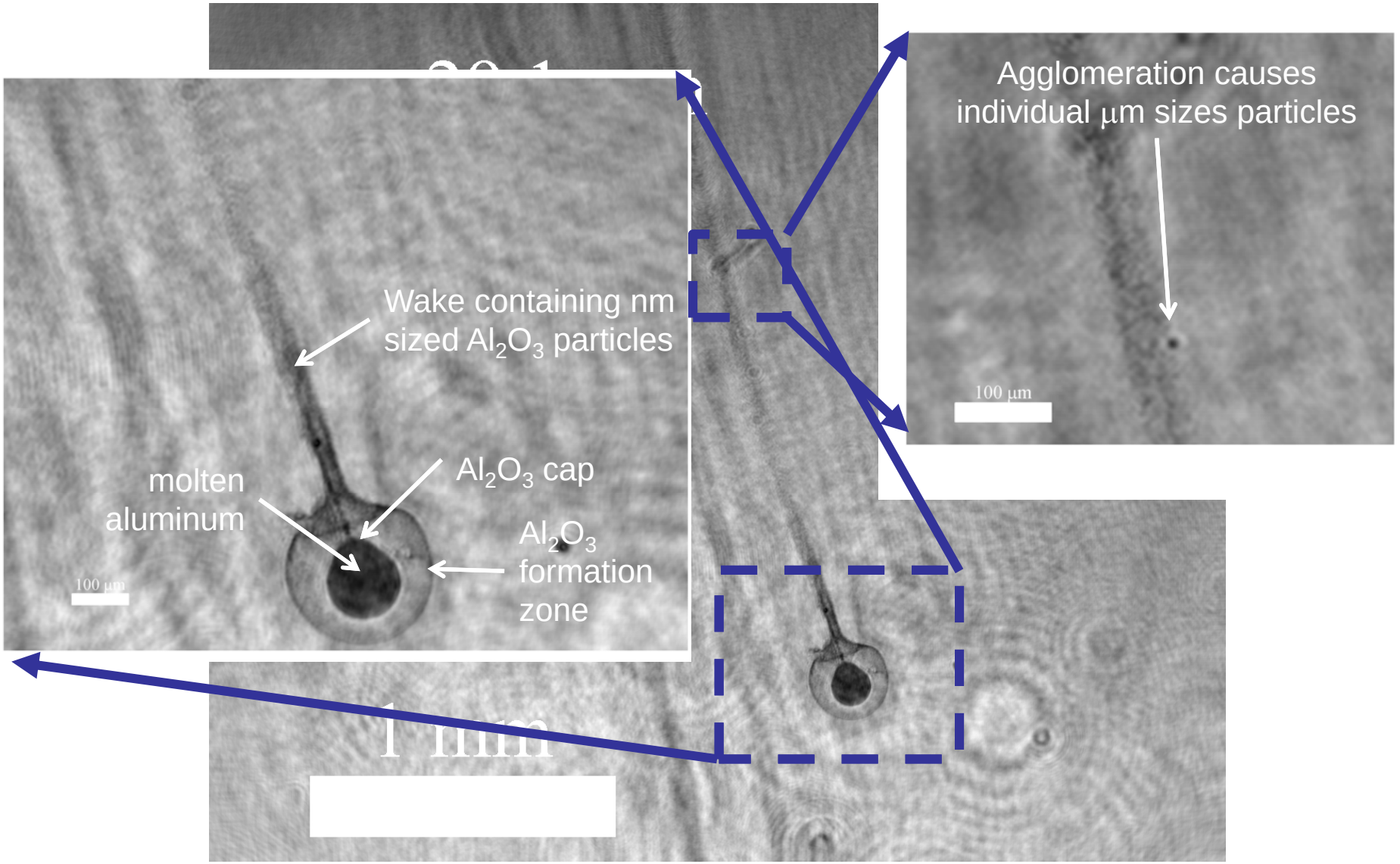

Conclusions

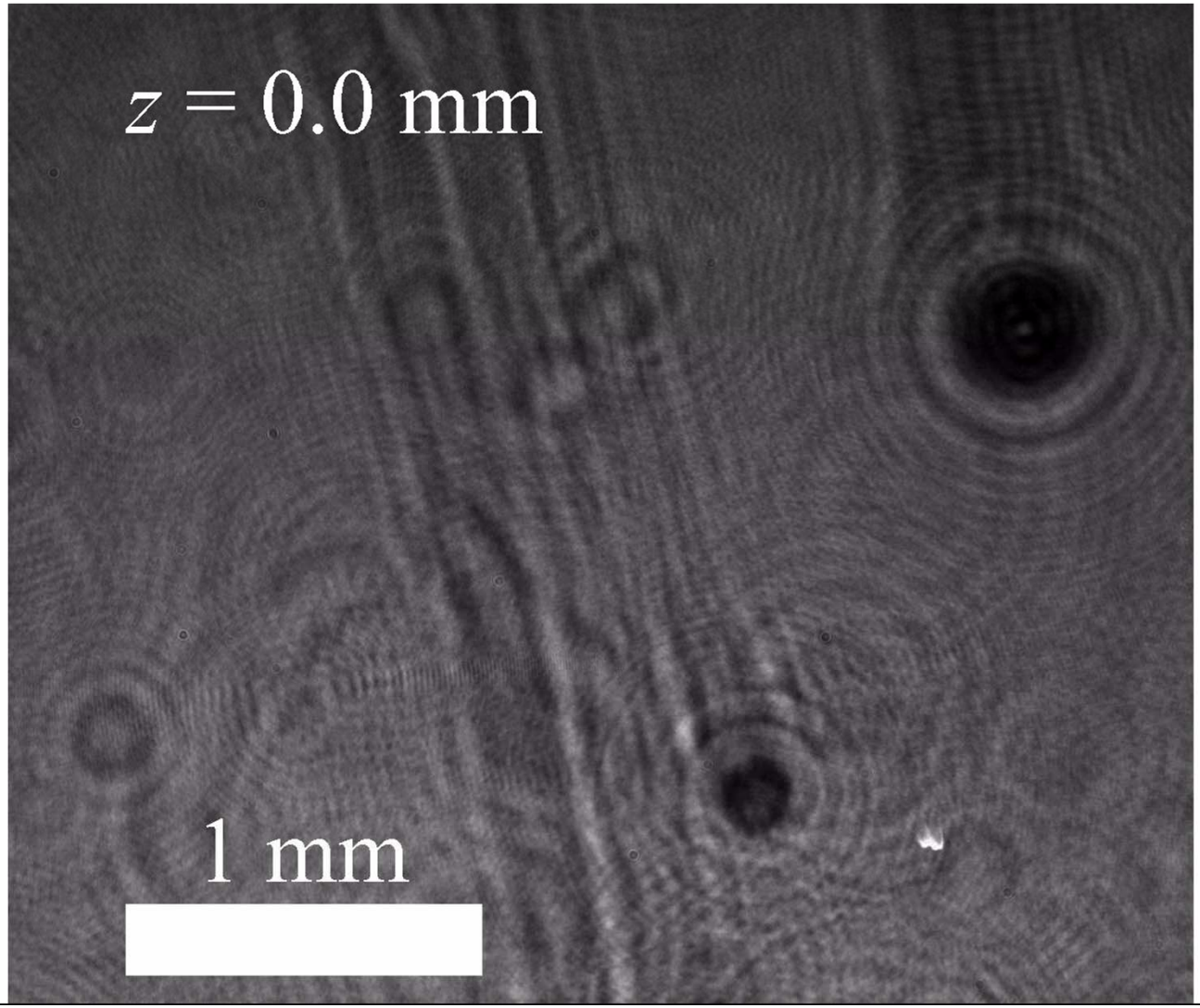

Developments in DIH enable quantitative 3D measurement of challenging multiphase flows with validated accuracy

Acknowledgements

- Phillip L. Reu at Sandia National Laboratories has provided significant collaboration throughout much of this development with particular emphasis on the high-velocity, shotgun experiments
- Significant thanks also goes to our collaborators at Purdue University
  - Professor Jun Chen and doctoral candidate Jian Goa
  - SNL sponsored work to develop particle detection algorithms
- Additional thanks to Thomas Grasser, Daniel Scoglietti, Lee Stauffacher, Luke Engvall, Sean Kearney, and many others….

Backup slides

Experimental configuration for *z* validation

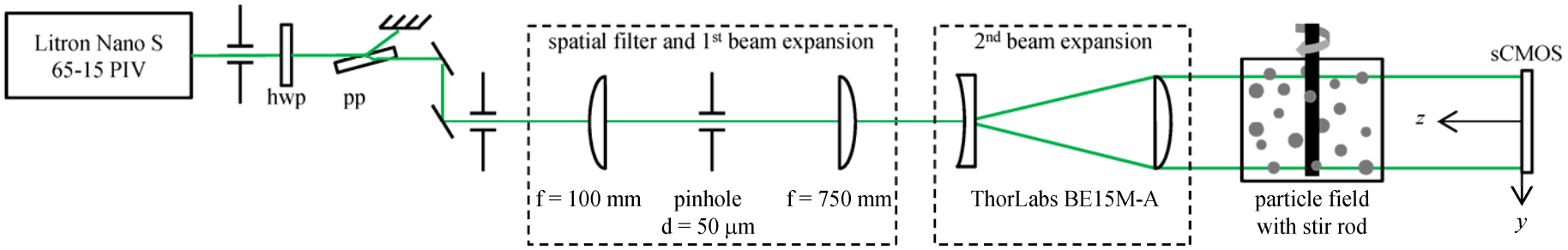

- Particles stirred by a rotating rod (r_0 = 1.58 mm, ω_0=100 rpm)
- Recorded at 15Hz with a LaVision sCMOS camera (2560 × 2160, 6.5 μm pixel pitch)

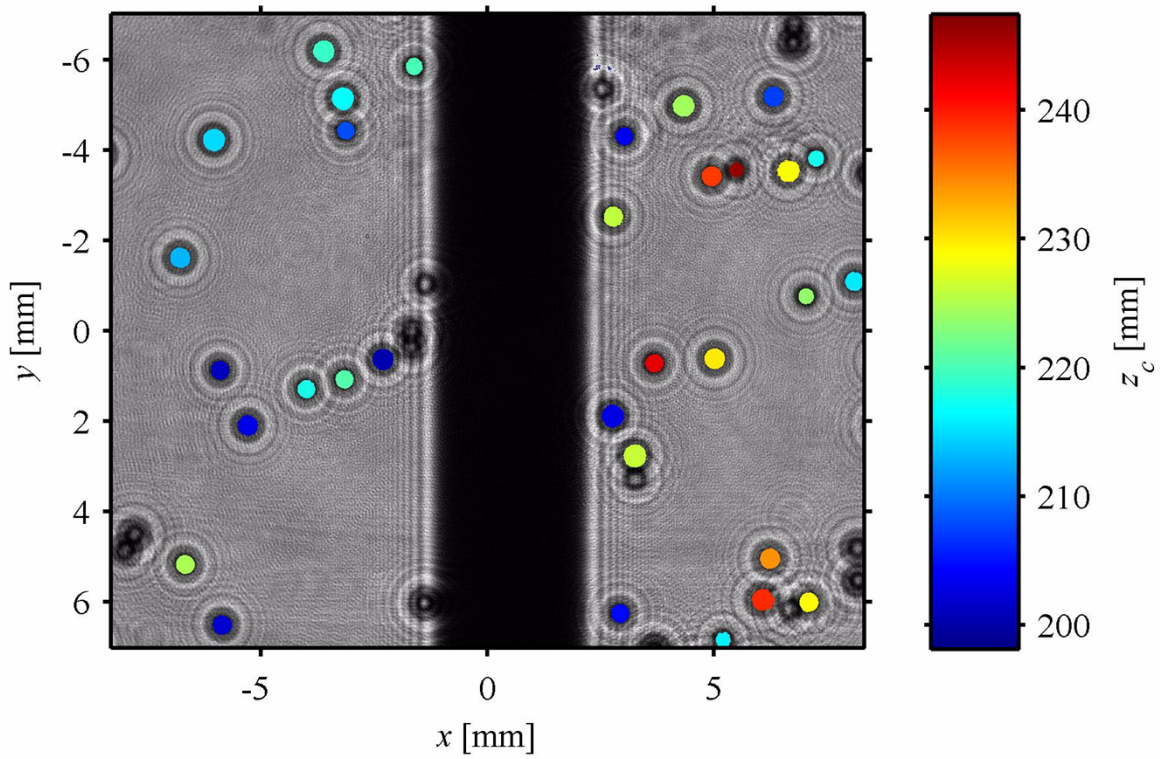

particles measured with the hybrid method, background shows the recorded holograms

Extraction of theoretical trajectory

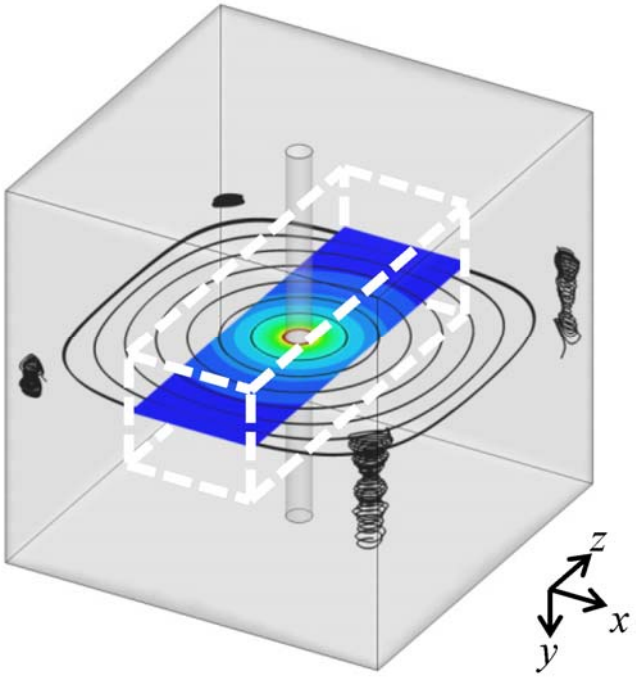

simulated flow field showing streamlines and total velocity contour within the center *x*-*z* plane of the field of view (dotted lines)

In the *x*-*z* plane, particles are expected to travel in near perfect circles

$$x(t) = r\cos(\omega t + \theta_0)$$

- Assuming measured *x*-positions have minimal error, curve fit → r, ω, θ_0

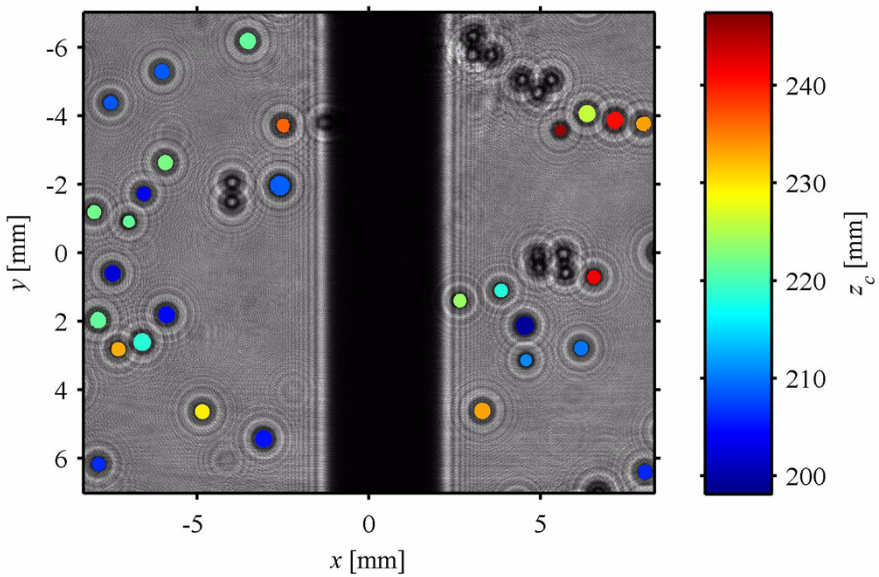

example in-plane trajectory

- Measured r = 5.04 mm, ω = 9.414 rpm
- At this r, simulation gives ω = 9.406 rpm

Comparison with measured results

Predicted *z*-trajectory: $z(t) = r\sin(\omega t + \theta_0)$ and $\Delta z(t) = r\omega\cos(\omega t + \theta_0)\cdot\Delta t$

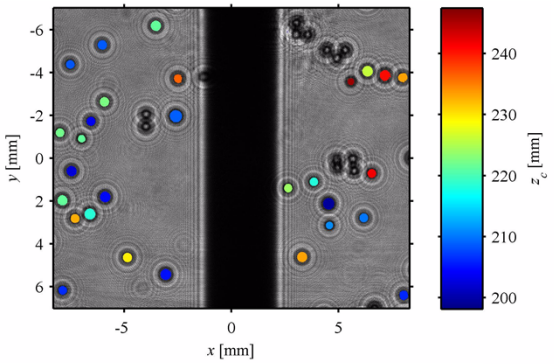

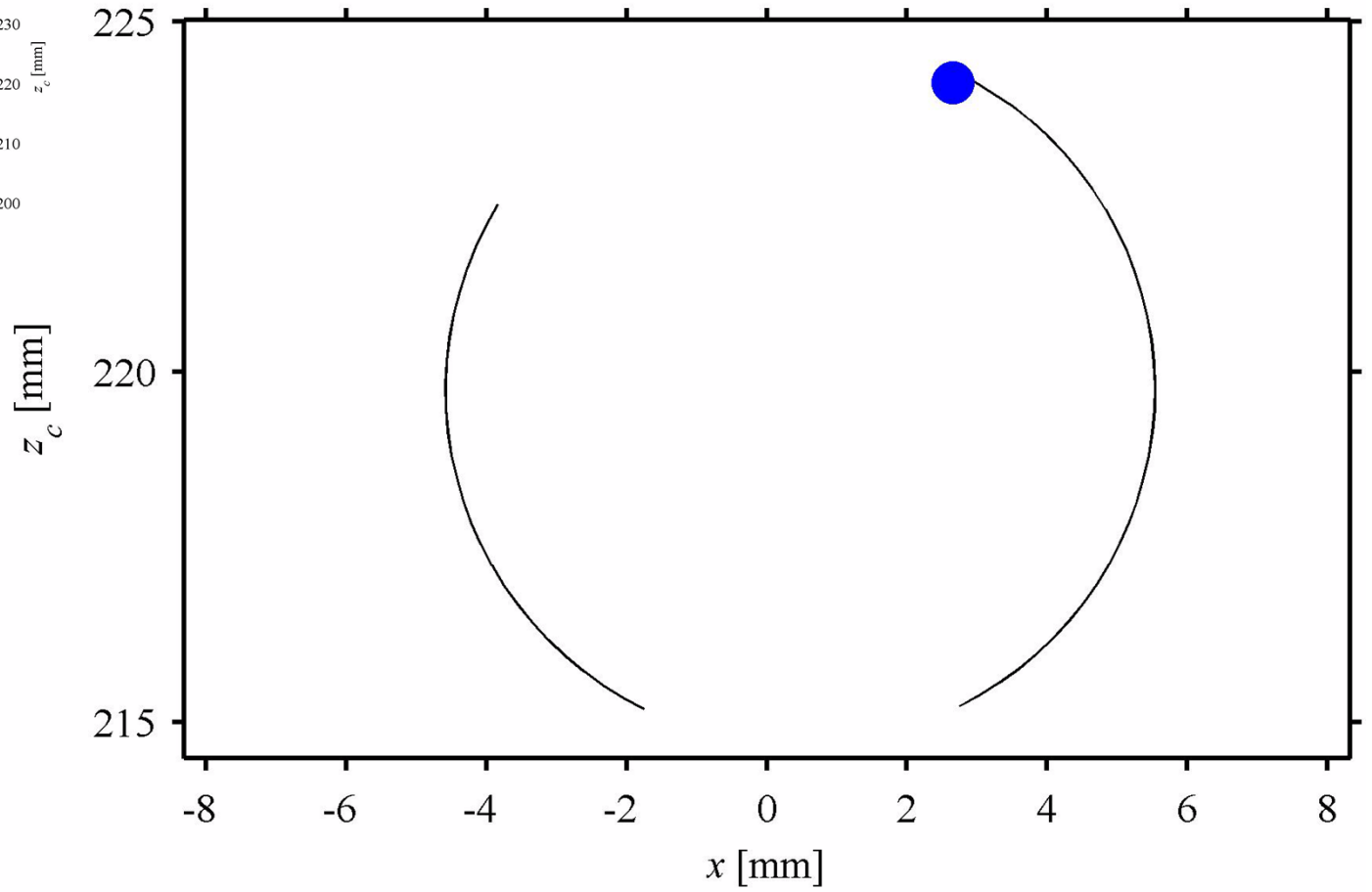

measured x-z trajectory vs. predicted

Conclusions

For all trajectories

- Error in measured z = -0.04 ± 1.51 mm
- Error in measured Δz = -0.03 ± 1.05 mm
  - Standard deviation of $2.3 \cdot \bar{d}$

Experiments repeated with smaller particles ($\bar{d} = 118 \mu m$, see paper for details)

- Error in measured z = -0.003 ± 0.379 mm
- Error in measured Δz = -0.001 ± 0.302 mm
  - Standard deviation of $2.6 \cdot \bar{d}$

Next steps:

- Compare results with alternative particle detection methods
- Use results to quantify effects of particle overlap and other experimental noise sources

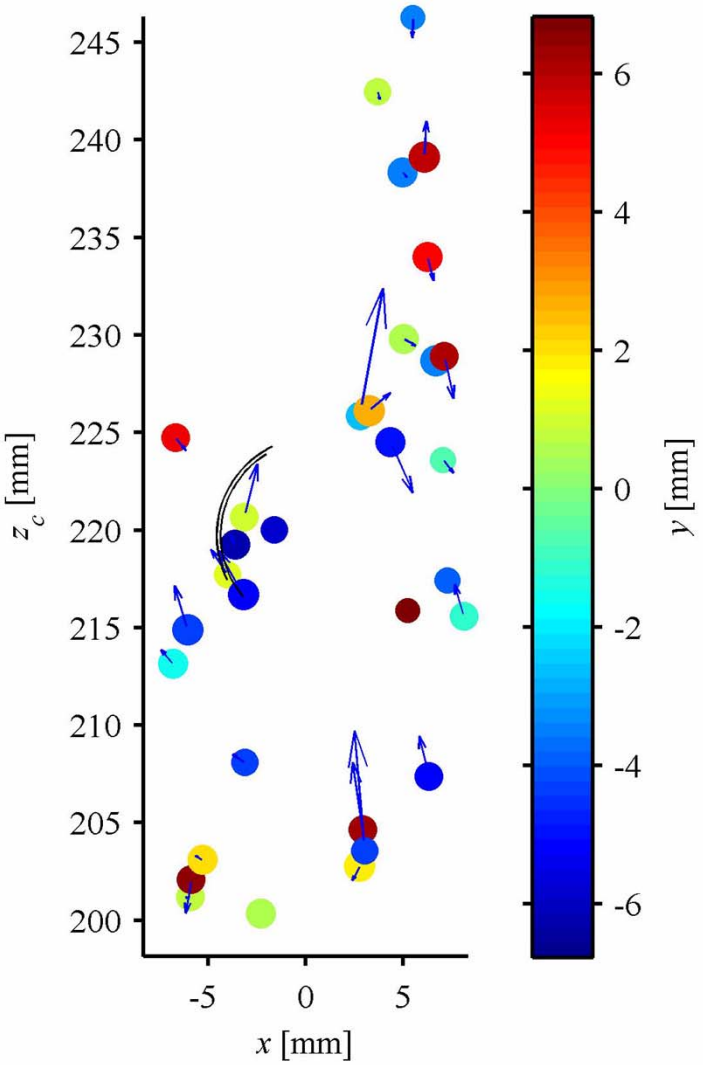

all measured x-z trajectories vs. predicted

3D, 3C fluid velocity measurements?

Sandia National Laboratories

Advantages:

- Simple optical setup requiring only one line-of-sight view
- Large depth of field (hundreds of mm possible)
- Particle sizes can be measured (if desired)

Challenges:

- High uncertainty in the *z*-direction
- Particle field must be relatively sparse providing only limited vectors
- Vectors at random positions
- Methods not as mature as PIV or even tomographic-PIV

Note: the literature contains many works on holographic-PIV. My own work has not been focused on these applications

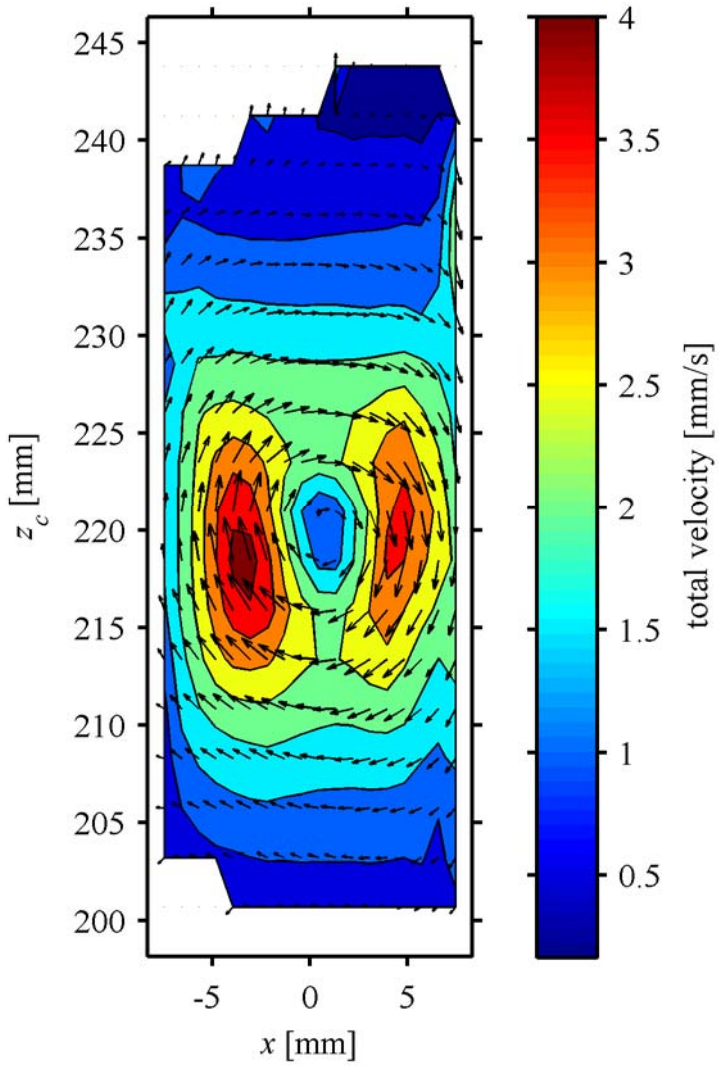

mean measured *x*-*z* velocities